

1 **Historical variation in normalized difference vegetation index**
2 **compared with soil moisture at a taiga forest ecosystem in**
3 **northeastern Siberia**

4 Aleksandr Nogovitcyn¹, Ruslan Shakhmatov^{1,2}, Tomoki Morozumi³, Shunsuke Tei^{4,5}, Yumiko
5 Miyamoto^{4,6}, Nagai Shin⁷, Trofim C. Maximov⁸ and Atsuko Sugimoto⁴

6 ¹Graduate School of Environmental Science, Hokkaido University, Sapporo, 060-0817, Japan

7 ²Slavic-Eurasian Research Center, Hokkaido University, Sapporo, 060-0809, Japan

8 ³National Institute for Environmental Studies, Tsukuba, 305-8506, Japan

9 ⁴Arctic Research Center, Hokkaido University, Sapporo, 001-0021, Japan

10 ⁵Forestry and Forest Products Research Institute, Tsukuba, 305-8687, Japan

11 ⁶Faculty of Agriculture, Shinshu University, Kamiina, 399-4598, Japan

12 ⁷Research Institute for Global Change, Japan Agency for Marine-Earth Science and Technology, Yokohama, 236-0001, Japan

13 ⁸Institute for Biological Problems of Cryolithozone, Siberian Branch of the Russian Academy of Sciences, Yakutsk, 677000,
14 Russia

15 *Correspondence to:* Atsuko Sugimoto (sugimoto@star.dti2.ne.jp)

16 **Abstract.** The taiga ecosystem in northeastern Siberia, a nitrogen-limited ecosystem on permafrost with a dry climate,
17 changed during the extreme wet event in 2007. We investigated the normalized difference vegetation index (NDVI) as a
18 satellite-derived proxy of needle production and compared it with ecosystem parameters such as soil moisture water
19 equivalent (SWE), larch foliar C/N ratio, $\delta^{13}\text{C}$ and $\delta^{15}\text{N}$, and ring width index (RWI) at the Spasskaya Pad Experimental
20 Forest Station in Russia for the period from 1999 to 2019. Historical variations in NDVI showed a large difference between
21 typical larch forest (unaffected) and the sites affected by the extreme wet event in 2007 because of high tree mortality at
22 affected sites under extremely high SWE and waterlogging, resulting in a decrease in NDVI, **although there was no**
23 **difference in the NDVI between typical larch forest and affected sites before the wet event.** Before 2007, the NDVI in a
24 typical larch forest showed a positive correlation with SWE and a negative correlation with foliar C/N. These results indicate
25 that not only the water availability (high SWE) in the previous summer and current June but also the soil N availability **likely**
26 increased needle production. NDVI was also positively correlated with RWI, resulting from similar factors controlling them.
27 However, after the wet event, NDVI was negatively correlated with SWE, while NDVI showed a negative correlation with
28 foliar C/N. These results indicate that after the wet event, high soil moisture availability decreased needle production, which
29 may have resulted from lower N availability. **Foliar $\delta^{15}\text{N}$ was positively correlated with NDVI before 2007, but after the wet**
30 **event, foliar $\delta^{15}\text{N}$ decreased.** This result suggests damage to roots and/or changes in soil N dynamics due to extremely high
31 soil moisture. **As a dry forest ecosystem, taiga in northeastern Siberia is affected not only by temperature-induced drought but**
32 **also by high soil moisture, led by extreme wet events, and nitrogen dynamics.**

33 **1 Introduction**

34 Boreal forests in northern regions of North America and Eurasia, including islands, occupy a large area, approximately 27 %
35 of the world's forest cover (FAO, 2020). Under conditions of increasing atmospheric CO₂ concentrations (e.g. Friedlingstein
36 et al., 2022), the role of taiga and other terrestrial ecosystems as carbon sinks becomes more important. Among the taiga
37 areas, Alaska, Canada, and Siberia are distinguished by permafrost, which is one of the main components of the global
38 carbon cycle. Under warming conditions, northern ecosystems respond differently to environmental changes depending on
39 the different biomes and regions, as mentioned below from remote sensing satellite observations. The normalized difference
40 vegetation index (NDVI), the most common remote sensing vegetation data, typically shows increasing trends (greening) in
41 arctic tundra but decreasing trends (browning) in many boreal forests (Bunn and Goetz, 2006; Verbyla, 2008; Berner and
42 Goetz, 2022; Miles and Esau, 2016). Observed greening at the tundra and taiga-tundra boundary can be associated with the
43 expansion of trees and shrubs to the north (Frost and Epstein, 2014; Tape et al., 2006; Shevtsova et al., 2020) and increases in
44 aboveground plant biomass (Goetz et al., 2005; Berner et al., 2013; Forbes et al., 2010). In turn, the browning of taiga can be
45 attributed to tree mortality and decreases in forest production because of droughts (Welp et al., 2007; Bunn and Goetz, 2006),
46 forest fires (Goetz et al., 2005), and extreme wet events (Famiglietti et al., 2021; Nogovitcyn et al., 2022). Nevertheless,
47 temporal changes in the NDVI of boreal forests are spatially heterogeneous and vary depending on different factors, such as
48 the plant vegetation types (Myers-Smith et al., 2020; Bunn and Goetz, 2006), stand density (Bunn et al., 2007; Dearborn and
49 Baltzer, 2021) and topography (Sato and Kobayashi, 2018). One of the most important factors controlling greenness is water
50 availability (Ruiz-Perez and Vico, 2020; Forkel et al., 2015). Overall, warming condition of boreal forests has positive effects
51 in wetter regions but negative effects on forest productivity in dry regions (e.g., Ruiz-Perez and Vico, 2020).

52 Siberian taiga is mainly covered with deciduous conifers ~~coniferous trees~~, larches, which grow under severe conditions, such
53 as continental climate, that is, cold winters, hot summers, low precipitation (Archibald, 1995), and limited nitrogen
54 availability (Popova et al., 2013; Kajimoto et al., 1999). Permafrost and seasonal ice are important sources of water for
55 larches during drought (Sugimoto et al., 2003; Sugimoto et al., 2002). These severe conditions make this ecosystem
56 vulnerable to environmental changes. ~~Under warming, permafrost may decline, which can trigger large amounts of carbon~~
57 ~~emissions (Schuur et al., 2015) and change the ecosystem.~~ In northeastern Siberia, the role of the taiga ecosystem and its
58 responses to climate change have been studied at the Spasskaya Pad Forest Station near Yakutsk over a long-term. ~~This larch~~
59 ~~forest is a net CO₂ sink; however, quantitative estimations of the flux from tower measurements and various models differ~~
60 ~~(Takata et al., 2017).~~ Over the past few decades, the ring width index (RWI) has decreased in this region as well as in other
61 continental dry regions, Alaska, Canada, and southern Europe, because of high temperature-induced droughts (Tei et al.,
62 2017). On the other hand, precipitation extremes, which are predicted to be more intensive and frequent (Douville et al.,
63 2021; Wang et al., 2021), can also negatively affect the forest. ~~Larch roots, which usually take up water from seasonal ice in~~

64 the active layer (above the permafrost) under dry conditions, can adapt to wet conditions by decreasing vertical distribution
65 (Takenaka et al., 2016). In addition to droughts, extreme wet events occur because of intensive precipitation, such as heavy
66 rainfall and snowfall. In this forest area, changes in winter precipitation may shift the forest phenology and production of soil
67 inorganic nitrogen, as demonstrated in snow manipulation experiments (Shakhmatov et al., 2022).

68 In northeastern Siberia, boreal forests have been affected by drought in the past because of the continental climate. However,
69 the extreme wet event in 2007, when soil moisture was the highest in the past century (Tei et al., 2013), because of large
70 amounts of rainfall and subsequent winter snowfall, which led to waterlogging in topographic depressions of the forest. This
71 extreme wet event was fatal for many trees in the forest, especially in the depressions (Iijima et al., 2014; Ohta et al., 2014).
72 These extremely moist conditions reduced CO₂ uptake by vegetation (gross primary production) and evapotranspiration
73 (Ohta et al., 2014). Evapotranspiration in this region is mainly controlled by the leaf area index (LAI) (Matsumoto et al.,
74 2008), suggesting a decrease in LAI in 2007 because of high tree mortality. In addition to high tree mortality, affected sites
75 are distinguished by a secondary succession of the understory and floor vegetation communities to water-resistant species
76 (Ohta et al., 2014). It was suggested that such sites in the forest generally emit methane, which makes the ecosystem a net
77 CH₄-source according to estimations of open-path eddy covariance measurements (Nakai et al., 2020). The wet event was
78 caused by continuous heavy precipitation, including extremely large snowfall. Snow manipulation experiments in the forest
79 showed the influence of interannual variation in winter precipitation on the phenology and production of soil inorganic
80 nitrogen (Shakhmatov et al., 2022). After the extreme moist conditions formed in 2005–2009 However, after the extreme wet
81 event, eddy-covariance flux measurements showed no significant trends in CO₂ exchange at the ecosystem scale (Kotani et
82 al., 2019). The affected sites are distinguished not only by high tree mortality but also by a secondary succession of the
83 understory and floor vegetation communities to water-resistant species, which may have compensated for the reduced water
84 and CO₂ fluxes (Ohta et al., 2014).

85 Boreal forests in northeastern Siberia have been affected by both drought and extreme wet events, as described above, which
86 involved complex changes in the forest environment. Tei et al. (2019a) demonstrated that larch trees, which died during the
87 extreme wet event, were affected by a previous drought. However, at the forest level, the NDVI was not related to gross
88 primary production in 2004–2014 (Tei et al., 2019b), and the NDVI of the larch forest damaged by waterlogging showed
89 insignificant trends in 2000–2019 and an insignificant correlation with climate data (Nagano et al., 2022). These phenomena
90 were attributed to waterlogging-induced changes in the understory and floor vegetation composition (Nagano et al., 2022; Tei
91 et al., 2019b), but they seem to be also related to changes in the conditions of the larch forest.

92 The high mortality of larches in 2007 could have been caused by two consecutive extreme events—drought and wetness (Tei
93 et al., 2019a). Severe drought and moist conditions in the forest lead to changes in the normalized difference vegetation index
94 (NDVI) (Tei et al., 2019b; Nagano et al., 2022), which is considered a proxy of vegetation productivity. However, gross

95 primary production (GPP) was found to be more related to the larch tree RWI in 2004–2014, but not to NDVI, because of
96 changes in the understory and floor vegetation composition (Tei et al., 2019b). Based on an investigation of spatial variations
97 in NDVI and foliar parameters in 2018, Nogoviteyn et al. (2022) found that affected sites with lower NDVI due to a smaller
98 number of living mature trees showed higher nitrogen and light availabilities (higher foliar C/N and $\delta^{13}\text{C}$, respectively) due to
99 low competition for resources. These favorable conditions can contribute to further succession. Although many studies have
100 been conducted in eastern Siberia, no study has focused on the relationships between historical NDVI and foliar parameters
101 in this region.

102 The taiga ecosystem in eastern Siberia is one of the most important biomes in the world and is vulnerable to climate
103 change. The purpose of this study was to understand how the larch forest in this region changed, particularly after the
104 extreme wet event in 2007, and what factors impacted the changes over the past two decades. Therefore, we investigated
105 historical variations in satellite-derived NDVI to evaluate changes in the forest, as the leaves of deciduous trees reflect the
106 condition of trees in each year. To understand the factors impacting forest changes, especially related to the extreme wet
107 event, NDVI data were compared with field-observed parameters in a typical larch forest, such as the RWI, soil moisture,
108 needle $\delta^{13}\text{C}$, $\delta^{15}\text{N}$, C/N, air temperature, and precipitation from 1998 to 2019.

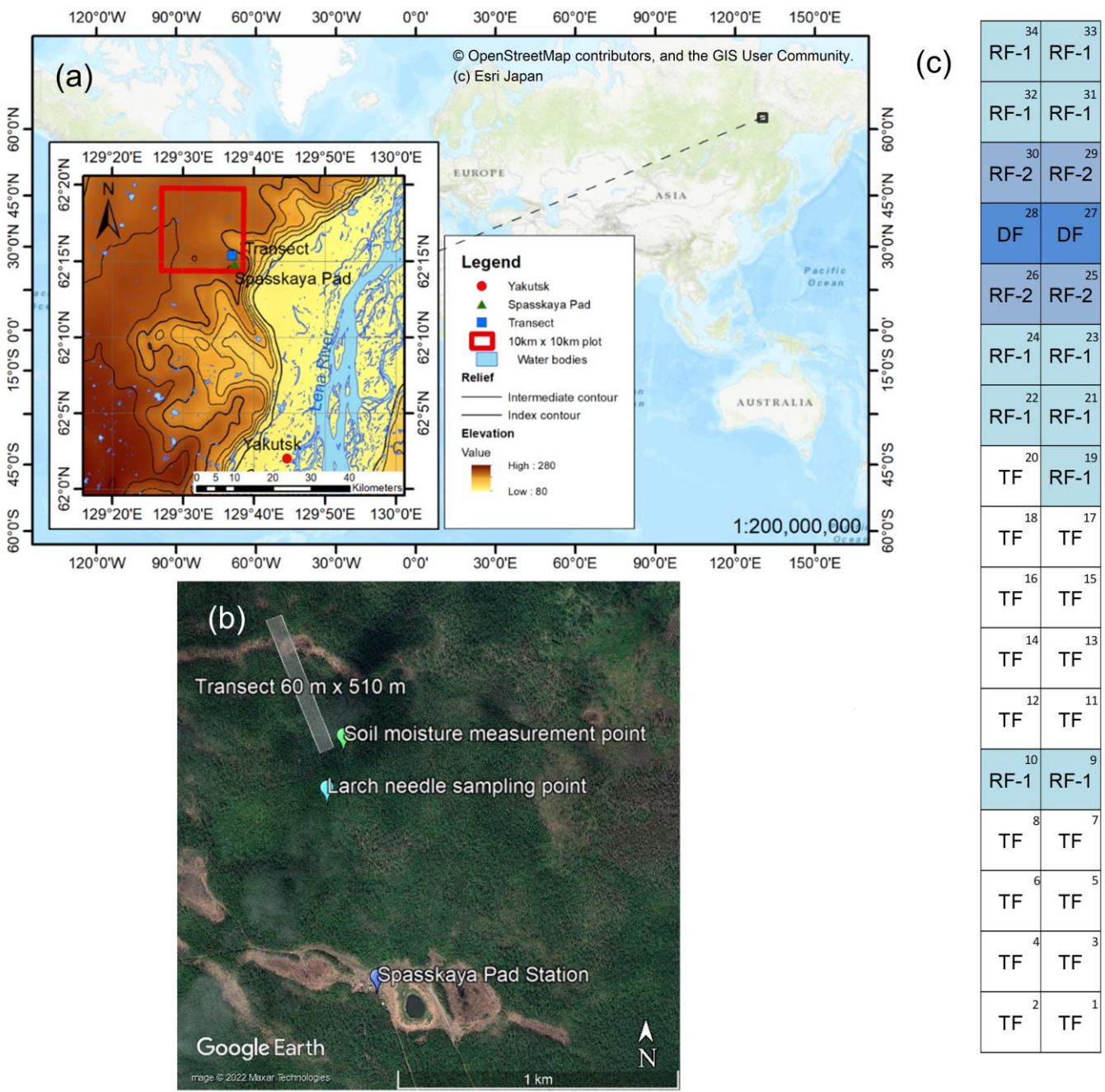
109 2 Materials and Methods

110 2.1 Study site

111 The study was conducted in the Spasskaya Pad Experimental Forest (62°15'18"N, 129°37'08"E, alt. 220 m a.s.l.), Institute
112 of Biological Problems of Cryolithozone, Siberian Branch of the Russian Academy of Sciences (IBPC SB RAS), near
113 Yakutsk, Russia (Fig. 1a). The region in Eastern Siberia is established on continuous permafrost and has a continental climate
114 (dry climate) with an extremely high annual temperature range. During the observation period from 1991 to 2020 at Yakutsk,
115 the average annual precipitation was 233 mm, and the average monthly temperature ranged from -37°C to +20 °C in cold
116 January and warm July, respectively. Dominant species is larch (*Larix cajanderi*) that is deciduous conifer (Abaimov et al.,
117 1998), mixed with broadleaved birch (*Betula pendula*), and the understory includes small shrubs, such as evergreen cowberry
118 (*Vaccinium vitis-idaea*) and deciduous bearberry (*Arctous alpina*), and grasses.

119 During the period from 2005 to 2007 (water years, from October to September), there was a large amount of precipitation
120 (307 ± 29 mm) continuously, which caused a significant increase in soil moisture (Sugimoto, 2019) and even waterlogging.
121 Consequently, an extreme wet event occurred in 2007, which damaged larch forests, resulting in high tree mortality and a
122 change in the composition of understory vegetation to moisture-tolerant grasses and shrubs in some areas, especially in
123 depressions (Iijima et al., 2014; Iwasaki et al., 2010; Ohta et al., 2014). In the summer of 2018, we set a 60 m \times 510 m
124 transect, which included areas unaffected and affected by the extreme wet event (Fig. 1a, b). The transect was divided into 30

125 \times 30 m plots (34 plots in total). Using these plots, we observed spatial variation in NDVI (Nogovitcyn et al., 2022). In this
126 study, we visually classified the forest conditions based on photographs. Four forest types were identified along the transect
127 (Fig. 1c): typical mature (TF; number of plots in the transect, $n = 17$), regenerating-1 (RF-1; $n = 11$), regenerating-2 (RF-2; n
128 = 4), and damaged (DF; $n = 2$) forests. The first TF showed no visible damage from the extreme wet event. The plots
129 discerned as regenerating forests RF-1, had many dead mature larches and formed forest gaps in the overstory where there
130 were a large number of young larches (seedlings and saplings with a height of up to 3 m) and shrubs. **Regenerating forests,**
131 **RF-2, contained more dead mature larches and more young larches compared to those in RF-1.** Damaged forests, DF, where
132 all mature trees died, was predominantly covered by moisture-tolerant grasses, and had much smaller numbers of young
133 larches than in RF-1 **and RF-2.** The DF plots were located on a depression in a trough-and-mound topography, and some
134 patches of the DF plots were flooded. **Regenerating forests RF-2 had moderate forest conditions between RF-1 and DF.**



135

136 **Figure 1.** (a) Location of the Spasskaya Pad Station (62°15'18"N, 129°37'08"E) and the study transect near Yakutsk in the topographic
137 map (modified from USGS/NASA Landsat 8 image) zoomed from a global map (Source: © OpenStreetMap contributors, © Esri Japan).
138 (b) Detailed view of the study area in the Spasskaya Pad Forest (Source: © Google Earth, © 2022 Maxar Technologies): locations of the
139 station, 60 m x 510 m transect, and points of soil moisture measurement and larch needle sampling for $\delta^{13}\text{C}$, $\delta^{15}\text{N}$, and C/N. (c) Scheme of
140 the transect with a total of 34 plots, which were divided into four forest types based on the level of forest damage (Nogovitcyn et al., 2022):
141 typical forests (TF), two types of regenerating forests (RF-1 and RF-2), and damaged forests (DF).

142 2.2 NDVI

143 The raster normalized difference vegetation index (NDVI) was computed based on the Landsat Collection-1 Level-2 image
144 products (<https://earthexplorer.usgs.gov/>) with a spatial resolution of 30 m using QGIS software (v. 3.2.2-Bonn):

145 $NDVI = (NIR - R) / (NIR + R)$,

146 where NIR and R are the near-infrared and red surface reflectance bands of the product, respectively. The image products
147 georeferenced to the WGS-84 UTM 52N coordinate system were selected according to the location of the study transect. The
148 NDVI value was extracted for each transect plot using the zonal **statistics** function. The transect plots, which consist of only
149 pixels attributed to quality pixels (clear terrain, low-confidence cloud, and low-confidence cirrus) in the quality assessment
150 bit index band according to Landsat Surface Reflectance product guides, were used in the analysis.

151 To investigate the historical variation in NDVI, we considered the seasonal maximum of the mean NDVI of the transect for
152 the long-time period from 1999 to 2019. The longest time-series data available for the study area has been obtained by the
153 Landsat 7 satellite with the Enhanced Thematic Mapper Plus (ETM+) image sensor since 1999. However, its sparse temporal
154 resolution (16 days) and scan-line corrector failure in 2003 forced the consideration of additional data from other satellites,
155 such as Landsat 5 Thematic Mapper (TM) (available until 2011) and Landsat 8 Operational Land Imager (OLI) (available
156 since 2013). Because the last two have different sensors in contrast to Landsat 7, NDVI values calculated from the TM and
157 OLI images were converted to ETM+ using the linear equations:

158 $NDVI_{ETM+} = 1.037 \cdot NDVI_{TM}$,

159 $NDVI_{ETM+} = 0.9589 \cdot NDVI_{OLI} + 0.0029$

160 developed by Ju and Masek (2016) and Roy et al. (2016), respectively, for boreal forests. Local parametrization of signals
161 from different sensors was not performed for our study site because of the insufficient overlap in the acquired images. We
162 identified that the selected and converted data were close to the 1:1 lines between Landsat 5 and 7 and between Landsat 7 and
163 8. For each year, a paired sample *t*-test was applied to determine the difference between the mean NDVI of the transect on
164 the observation days. In the case of statistically insignificant differences among observation days, we selected the day with
165 the highest number of quality pixels.

166 To verify the historical variation in NDVI of the transect, a larger area, 10 km × 10 km (hereafter, the 10-km plot), including
167 the Spasskaya Pad Forest, was used for comparison with the transect (the center of the 10-km plot was located at 62°17'4"N,
168 129°32'4"E; Fig. 1a). For each observation day, the mean NDVI of the 10-km plot was calculated using only quality pixels
169 using ENVI 5.1 (L3Harris Technologies, USA). For each year, the seasonal maximum NDVI of the 10-km plot was
170 determined as the highest mean NDVI among observation days, on which the number of quality pixels were more than 50 %
171 (total, 111,556 pixels). The seasonal maximums of the transect and 10-km plot showed the same day for about three-quarters
172 of the study period (15 years among 21) and showed a different day in six years (Table S1): 2006 (7 August and 29 July),
173 2007 (1 and 25 July), 2010 (1 and 15 July), 2011 (5 and 12 August), 2015 (23 and 31 July), and 2019 (1 and 9 July). The
174 averaged NDVI values of the 10-km plot, transect, and each forest type (TF, RF-1, RF-2, and DF) in the transect are shown
175 in Fig. 2a and 2b.

176 The NDVI data of larch forest, which is deciduous, quickly increases in early summer, when the NDVI is mostly stable (e.g.,
177 Huete et al., 2002). This stable NDVI continues for more than 1.5 months (typically from July to mid-August), although the
178 time period depends on the weather and soil moisture conditions. Seasonal maximum NDVI was identified during this
179 period. Although the data acquisition days were limited because of the low temporal resolution and cloud coverage, more
180 than three days of data were acquired by combining three satellite images, and seasonal maximums were determined, except
181 for in 1999 and 2003. These two years had only one data acquisition day, on 27 August 1999 and 21 July 2003, and both data
182 points were recognized as the seasonal maximum.

183 **2.3 Ecosystem and climate parameters**

184 Several ecosystem parameters have been observed since 1998 in typical forests. To monitor the physiological response of
185 larch to environmental changes, the C and N isotopic compositions ($\delta^{13}\text{C}$ and $\delta^{15}\text{N}$, ‰), and the ratio of C to N content (C/N)
186 of larch needles have been observed since 1999, except in 2012, at the site 200 m south of the transect (Fig. 1b). The $\delta^{13}\text{C}$
187 and $\delta^{15}\text{N}$ are calculated by:

188
$$\delta^{13}\text{C} \text{ (or } \delta^{15}\text{N}) = (R_{\text{sample}}/R_{\text{std}} - 1) \times 1000 \text{ (‰),}$$

189 where R_{sample} and R_{std} are isotope ratios ($^{13}\text{C}/^{12}\text{C}$ or $^{15}\text{N}/^{14}\text{N}$) of the sample and standard, respectively, and standards are
190 Vienna PeeDee Belemnite for C and atmospheric N₂ for N. The foliar $\delta^{13}\text{C}$ reflects the physiological condition of
191 photosynthesis and is widely applied to indicate plant water use efficiency (Farquhar et al., 1989). The $\delta^{13}\text{C}$ value of plant
192 tissue (e.g., leaf) is expressed using the following equation:

193
$$\delta^{13}\text{C} = \delta^{13}\text{C}_{\text{atm}} - a - (b - a) (C_i/C_a),$$

194 where $\delta^{13}\text{C}_{\text{atm}}$ is the C isotopic composition of atmospheric CO₂, a (4.4‰) and b (27‰) are isotope fractionations of the
195 diffusion and photosynthetic reaction, and C_i and C_a are intercellular and atmospheric CO₂ concentrations. The foliar $\delta^{13}\text{C}$
196 becomes high when higher irradiance and lower stomatal conductance are observed. At our study site, lower and higher $\delta^{13}\text{C}$
197 values of larch needles were typically due to wet and drought conditions. The foliar $\delta^{15}\text{N}$ is a physiological indicator of the N
198 source for a plant (Evans, 2001), which can vary depending on numerous physiological and environmental factors. The foliar
199 C/N represents the N status of a plant (Liu et al., 2005).

200 Larch needles were collected from four to eight young larch trees in August every year. We collected them from the same
201 trees (sample trees) every August, and these trees are located nearby to each other. Four stems were obtained from each tree,
202 and the needles from each tree were mixed and analyzed at Kyoto University (samples for 1999–2003) and Hokkaido
203 University (samples after 2004) using Conflo systems (EA 1108 and Delta S, and Flash EA 1112 and Delta V, Thermo Fisher
204 Scientific, at Kyoto and Hokkaido Universities, respectively). Analytical precisions (standard deviation) of the C and N
205 content measurements were better than 0.3% and 0.1%, respectively, and those for the isotopic compositions $\delta^{13}\text{C}$ and $\delta^{15}\text{N}$
206 were better than 0.2‰. The details of sampling, sample preparation and laboratory analyses of C and N contents and their

207 isotope compositions using the EA-IRMS system are described in Fig. S1. The details of the average calculations are shown
208 in Fig. S1 and S2. In 2015, there were no data on the $\delta^{15}\text{N}$ and N content.

209 For more than 100 years, until 2016, larch ring-width index (RWI) **indicating wood growth dynamics** was estimated by
210 detrending and standardizing the raw time-series width data obtained from the collected paired cores (Tei et al., 2019b; Fan et
211 al., 2021). The RWI data used for analysis are shown in Table S2.

212 Soil moisture was measured using time-domain reflectometry (TDR), and the soil moisture water equivalent (SWE; the
213 amount of liquid water contained within the soil layer, mm) in the 0–60 cm soil layer was obtained for 1998–2019 in June,
214 July, and August using the method described by Sugimoto et al. (2003) (near the transect; Fig. 1b). There were no data for
215 June of 2002 and 2011 and August of 2003. The details of the intra- and inter-annual variations in SWE are shown in Fig. S3.
216 Among the climate variables, summer air temperature and precipitation datasets recorded by the meteorological station at
217 Yakutsk (62.02° N, 129.72° E) were obtained from the All-Russia Research Institute of Hydrometeorological Information -
218 World Data Centre (RIHMI-WDC) website (<http://aisori-m.meteo.ru/>).

219 **2.4 Statistical analysis**

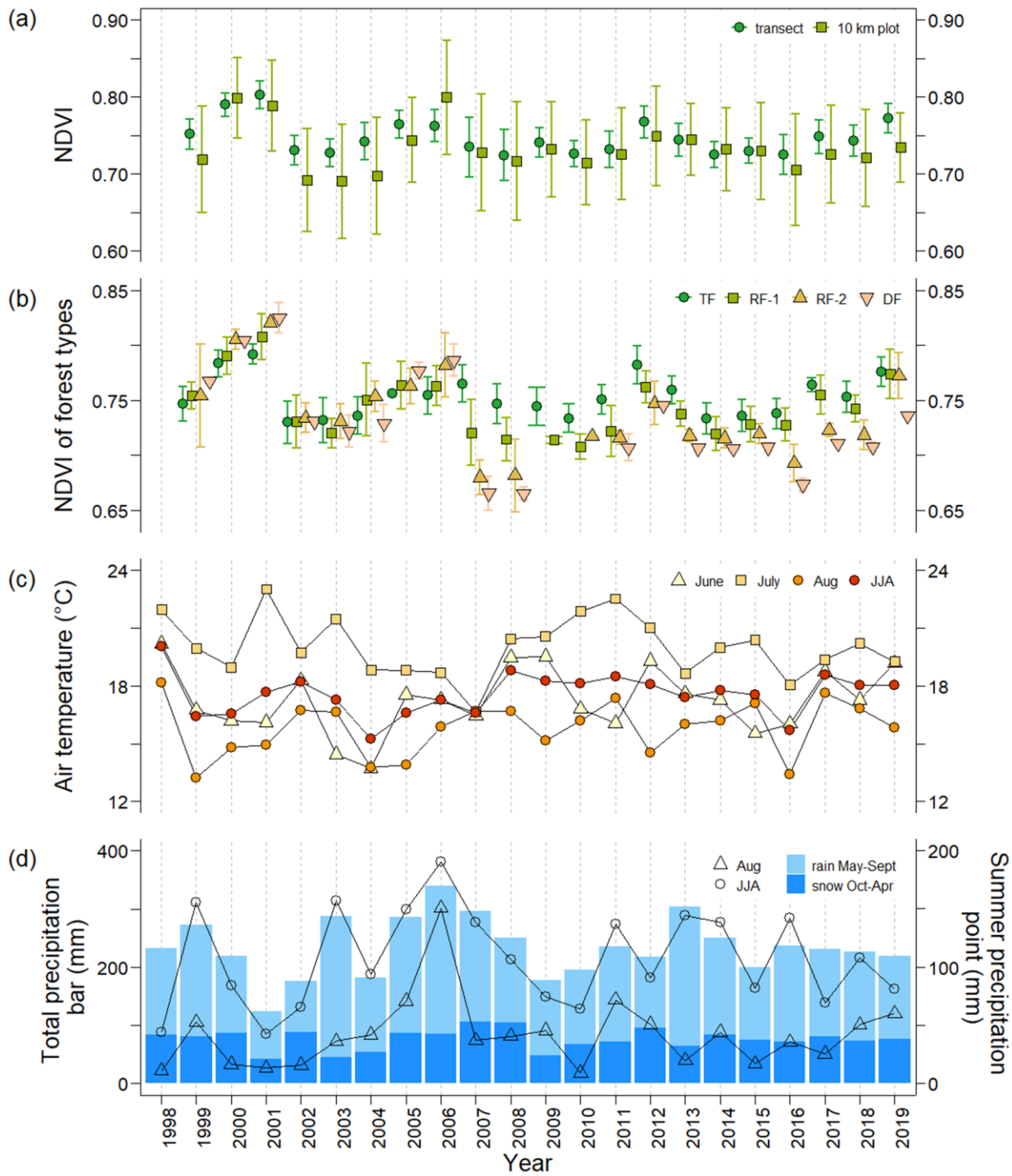
220 All statistical analyses were carried out using R statistics v.4.1.3 (R Core Team). Relationships between datasets were
221 investigated using a simple linear regression model (function “lm”) and a Pearson correlation test (“cor.test”), **the most**
222 **common statistical test based on the method of covariance**. Trends of NDVI change in 1999–2019 were estimated using the
223 Mann–Kendall test (package “trend”, function “mk.test”). Differences in NDVI among four forest types (TF, RF-1, RF-2 and
224 DF) were determined using Kruskal–Wallis test (“kruskal.test”) with pairwise Wilcoxon rank sum test
225 (“pairwise.wilcox.test”). **The criteria for applying a particular test were the data distribution type (normal or non normal) and**
226 **the relation of the data variances to each other (equal or unequal): Student’s *t* test, both datasets have “normal” distributions**
227 **and “equal” variances; Welch’s *t* test, “normal”, “unequal”; and Wilcoxon rank sum test, “non normal”, “unequal”. Data**
228 **normality and variance equality were checked using the Shapiro–Wilk test and *F* test.** The results of the statistical tests are
229 shown in the Supplemental (Table S3–S9). The models and tests described by levels of statistical significance (*p*-values) less
230 than 0.05 and 0.1 were considered to be “significant” and “moderately significant”, respectively.

231 **3 Results**

232 **3.1 Year-to-year variation of seasonal maximum NDVI**

233 Fig. 2a shows the historical variation in the seasonal maximum NDVI of the TF and the 10-km plot from 1999 to 2019. Both
234 NDVI time series varied similarly. The seasonal maximum of each year was observed from 25 June to 13 August, except for
235 1999 (shown in Table S1). The maximum transect NDVI in 1999 was observed on 27 August (0.75 ± 0.02 , $n = 34$) because

236 the Landsat data in 1999 were limited to the latter half of August. The mean seasonal maximum NDVI for the transect varied
237 between 0.72 and 0.80. During the period from 1999 to 2001, the NDVI of the transect was high from 0.75 ± 0.02 ($n = 34$) to
238 0.80 ± 0.02 ($n = 34$) (Fig. 2a), but in 2002 and 2003, the NDVI was much lower (0.73 ± 0.02 , $n = 34$) than that in 2001. From
239 2003 to 2006, NDVI again increased from 0.73 ± 0.02 ($n = 34$) to 0.76 ± 0.02 ($n = 34$). During the wet event in 2007–2008,
240 the NDVI decreased to 0.73 ± 0.04 ($n = 34$). After 2009, NDVI was higher than that in 2008 (0.72 ± 0.03 , $n = 34$), except in
241 2016 (0.72 ± 0.03 , $n = 31$).



242

243 **Figure 2.** The temporal variations from 1999 to 2019 in (a) seasonal maximum NDVI averaged for the plots in the transect and the
244 representative 10-km forest plot calculated from available Landsat 5, 7, 8 images; (b) NDVI of four forest types, typical mature forest (TF),
245 regenerating forests (RF-1 and FR-2), and damaged forest (DF); (c) mean air temperature in June, July, August and whole summer period
246 JJA (June-July-August); (d) the amount of precipitation during previous October-current April (snow) and current May-September (rain)
247 shown with blue bars, in August and whole summer period JJA (June-July-August) shown with triangles and circles. Both the mean NDVI
248 of the 10-km plot and the transect decreased from 1999 to 2019 (-0.0009 and -0.0010 year⁻¹, respectively), but not with statistically
249 significant trends. Generally, the mean NDVI in the transect was higher than that in the 10-km plot, except for 2000 and 2014.

250 **3.2 NDVI of each forest type**

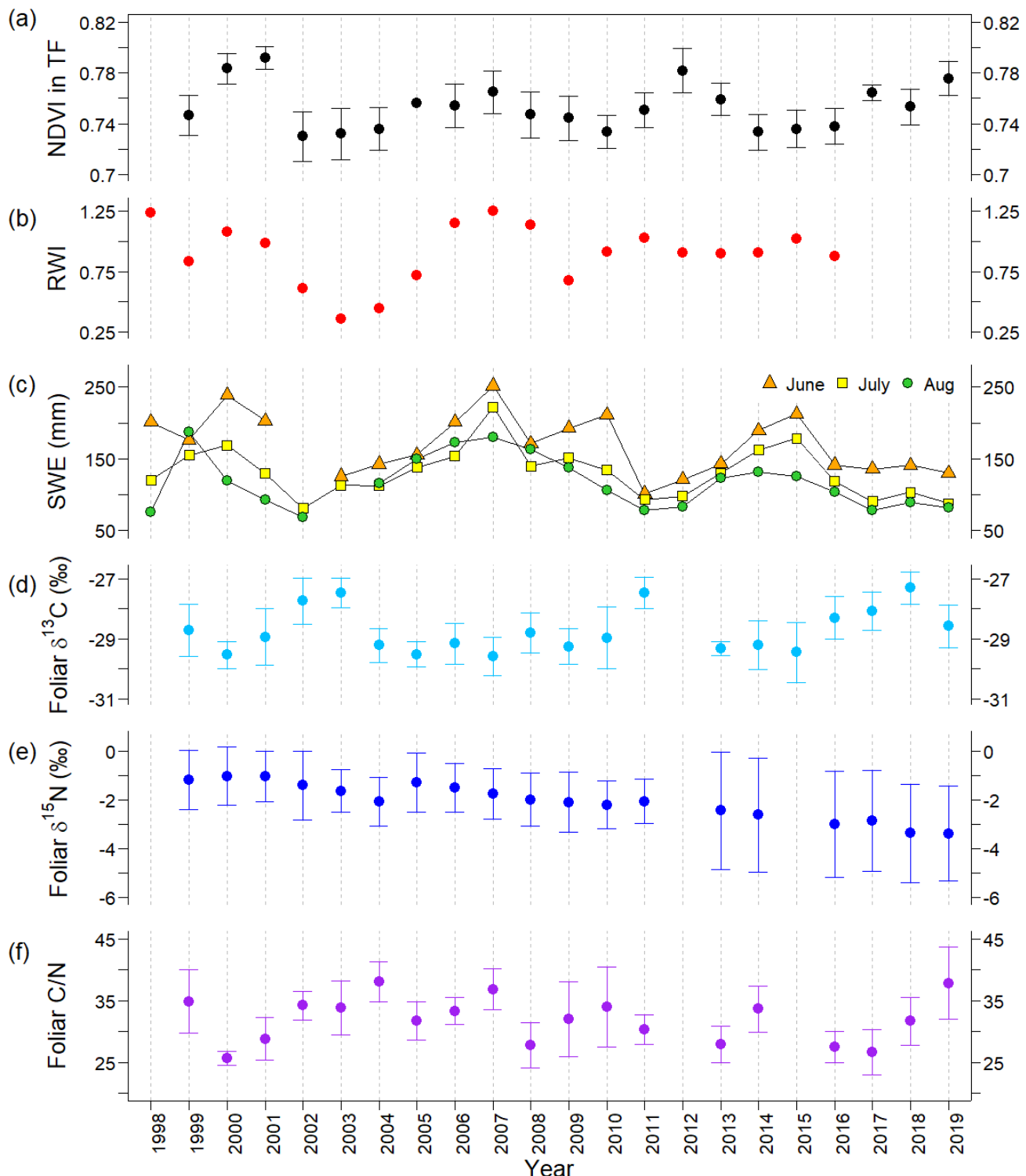
251 The NDVI time series for four forest types (typical forest TF, regenerating forests RF-1 and RF-2, and damaged forest DF) in
252 the transect during 1999–2019 are shown in Fig. 2b. As shown in Fig. 2b and 3a, before 2007, the NDVI of TF during 1999–
253 2001 (0.75 ± 0.02 to 0.79 ± 0.01 , $n = 17$) was higher than that in the subsequent period, 2002–2006 (0.73 ± 0.02 to $0.75 \pm$
254 0.02 , $n = 17$). In 2002, there was a significant decrease in the TF NDVI, which remained low between 2002 and 2004 (Fig.
255 2b and 3a). During 1999–2006, the NDVI values of the four types were close to each other, but after the wet event, NDVI
256 values noticeably differed among the forest types (Fig. 2b). In 2007, the NDVI of TF (0.76 ± 0.02 , $n = 17$) was the highest,
257 and those of the other three types decreased in the order of RF-1 (0.72 ± 0.03 , $n = 11$), RF-2 (0.68 ± 0.02 , $n = 4$), and DF
258 (0.67 ± 0.02 , $n = 2$) (Fig. 2b). In 2008, the NDVI decreased slightly and showed the same order of forest types as that in
259 2007. After 2009, the difference among the forest types, especially between TF and DF, remained, although it was smaller
260 than that in 2007.

261 **3.3 NDVI of the typical forest and ecosystem parameters of the study site**

262 To consider the historical variation in the NDVI of typical forests in our study area, the TF NDVI and observed parameters
263 were compared (Fig. 2 and 3). In Fig. 4, the linear relationships between NDVI and other parameters were investigated for
264 two different time periods, before (1999–2006) and after (2008–2019), to compare them.

265 **3.3.1 Climate parameters (temperature and precipitation) at Yakutsk**

266 Interannual variations in climatic parameters, such as air temperature and precipitation, from 1999 to 2019 are displayed in
267 Fig. 2c and 2d. The average air temperature in June–August (summer temperature) was relatively high in 1998, 2001–2002,
268 and 2008–2012 (Fig. 2c). The TF NDVI showed no correlation with summer temperature. The amount of annual water
269 precipitation (from October to September) for the period from 1991 to 2020 averaged approximately 233 ± 47 mm. As shown
270 in Fig. 2d, larger water year precipitation, that is, precipitation higher than 280 mm (one standard deviation above the mean
271 for 1991–2020), was observed in 2003 (287 mm), 2005–2007 (285, 340, and 296 mm), and 2013 (304 mm). The amount of
272 water precipitation in 2001 (124 mm) was the lowest during the observation period. The drought year (2001) showed a high
273 TF NDVI value. Consecutive wet years in 2005–2007 showed slightly higher TF NDVI values, but there was no correlation
274 between the water year precipitation and NDVI.



275

276 **Figure 3.** The temporal variations in ecosystem parameters observed during 1998–2019 at the typical forest (TF): (a) NDVI, (b) larch ring
 277 width index (RWI), (c) soil moisture water equivalent (SWE) at the depth of 0–60 cm in June, July, and August, (d) average foliar $\delta^{13}\text{C}$, (e)
 278 $\delta^{15}\text{N}$, and (f) C/N ratio. Error bars represent standard deviations. There were no data for NDVI in 1998, RWI during 2017–2019, June SWE
 279 in 2002, August SWE in 2003, foliar $\delta^{13}\text{C}$ in 1998 and 2012, and foliar $\delta^{15}\text{N}$ and C/N in 1998, 2012, and 2015.

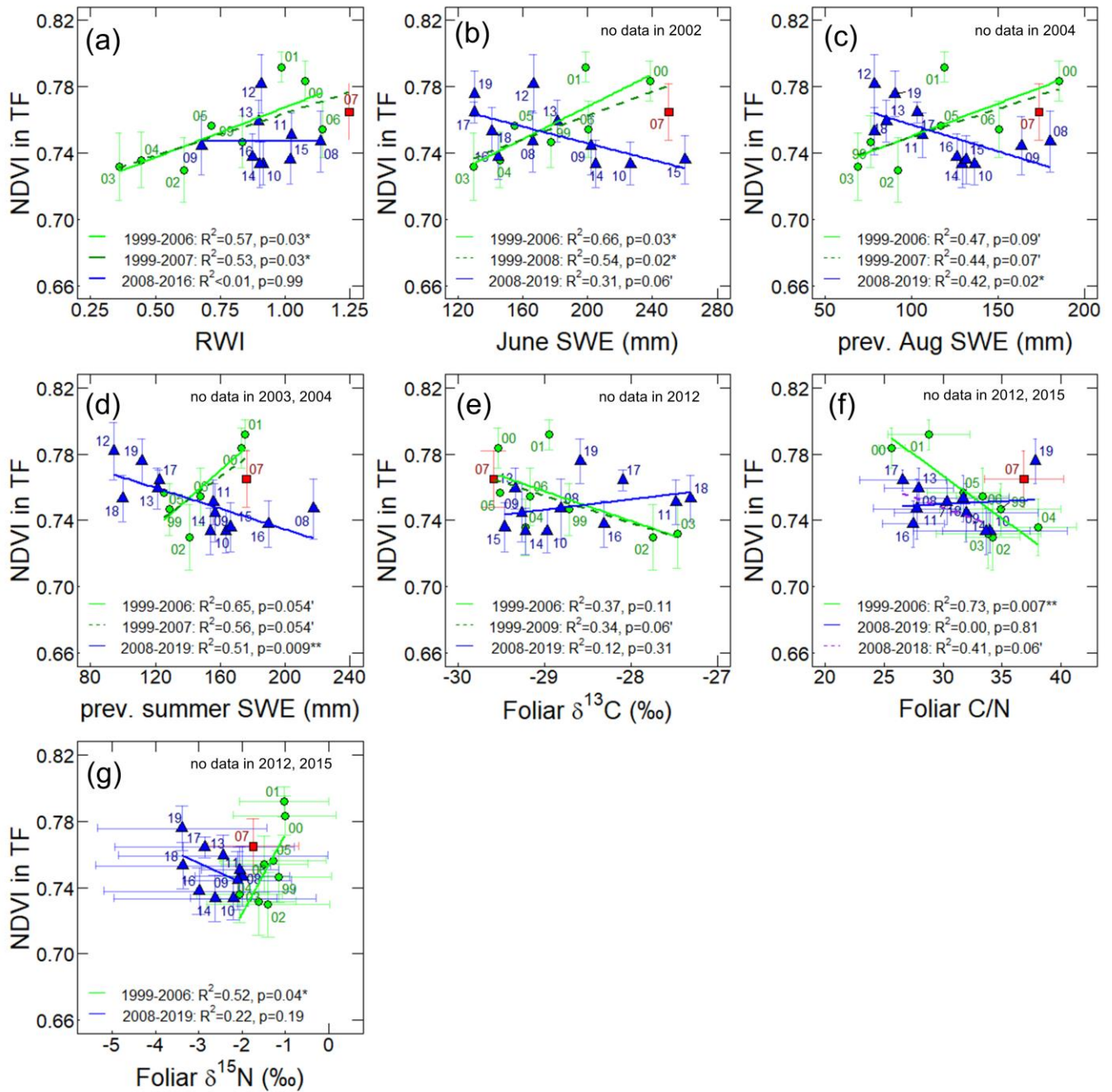


Figure 4. The relationships between the TF NDVI in transect and (a) larch RWI during 1999–2016, the monthly average of SWE (mm) in (b) June and (c) the previous August, (d) averaged monthly SWE for June–August of the previous year, (e) foliar $\delta^{13}\text{C}$, (f) C/N, and (g) $\delta^{15}\text{N}$ during 1999–2019. The green circles, red square, and blue triangles show data points during 1999–2006, 2007, and 2008–2019, respectively. Labels nearby the data points are observation years of the TF NDVI. Horizontal and vertical error bars represent standard deviations. Green and blue solid lines show linear regressions for 1999–2006 (before the wet event) and 2008–2019 (after the wet event), respectively, and dark green and purple dotted lines represent other periods. p -values and R^2 describe the significance and coefficient of determination of the regression models, respectively.

3.3.2 RWI at the typical forest

The larch RWI showed a trend similar to that of the transect TF NDVI during 1999–2007 (Fig. 3a and b). The RWI and

average TF NDVI showed high values in 2000–2001 (0.98–1.08 and 0.78–0.79) followed by low values in 2002–2003 (0.36–0.61 and 0.73); the RWI in 2003 was the lowest for the whole observation period. Subsequently, both parameters increased by 2007 (1.25 and 0.76). After 2007, these two parameters exhibited different behaviors. During the period from 2010 to 2013, a one-year time lag was observed in the TF NDVI: there was an increase in RWI from 2009 to 2011, a decrease in 2012, and one year later, from 2010 to 2012, the TF NDVI increased and then decreased in 2013. Statistically, the temporal correlation between the TF NDVI and RWI was positive at a ~~moderately~~-significant level during 1999–2016 ($r = 0.47, p < 0.05$; Table S7), with a ~~stronger~~ significant positive correlation before 2007 ($r = 0.76, p < 0.05$; Fig. 4a, Table S5) and an insignificant negative correlation after 2007 (Fig. 4a, Table S6).

3.3.3 Soil moisture water equivalent at the typical forest

The time series of the SWE and TF NDVI showed different correlations in the early and late halves of the observation period (Fig. 3a and 3c). During 1999–2007, the averaged SWE for June–August (hereafter, summer SWE) and the TF NDVI mostly showed similar trends. High values of the TF NDVI in 2000 and 2001 corresponded to high values of the SWE in the current June (239 and 202 mm) and in the last summer (173 and 176 mm in 1999 and 2000). These high values of TF NDVI and SWE were followed by low values during the drought period in 2002–2003. Subsequently, as summer SWE increased from 2004 (124 mm) to 2007 (218 mm), the TF NDVI also increased. ~~Therefore, before 2007, the TF NDVI showed the lowest values during the dry years, but the highest values were observed in the wet years (Table 1).~~ For the period from 2008 to 2019, the correlation between the TF NDVI and summer SWE was negative, with a one-year time lag in the SWE (Fig. 3a and 3c). A low summer SWE value was observed in 2011 (91 mm), and a high TF NDVI value was observed in the subsequent year, 2012. After 2016, the TF NDVI showed an increasing trend, whereas the SWE decreased from 2015 to 2019. Statistically, the TF NDVI showed positive correlations with the SWE in the current June ($r = 0.83, p < 0.05$) and the previous summer ($r = 0.79, p < 0.1$), including the previous July ($r = 0.82, p < 0.05$) and previous August ($r = 0.69, p < 0.1$), during the period from 1999 to 2006 (Fig. 4b–d and S4d; Table S5). However, after 2008, TF NDVI showed negative correlations with the SWE in the previous ($r = -0.65, p < 0.05$) and current ($r = -0.73, p < 0.01$) summer, at a stronger significance level (Fig. 4b–d and S4a–e; Table S6). During and after 2007, there was no change in the TF NDVI; slightly damaged RF-1 showed a decrease in NDVI to levels similar to those observed during the 2002 drought (Fig. 2b).

315 **Table 1.** Mean and standard deviation of seasonal maximum NDVI of all plots in the TF and RF 1 in the periods before
 316 (1999–2006), during (2007), and after (2008–2019) the extreme wet event. Averaged NDVI was also calculated for wet and
 317 dry periods before the event. Different letters in the superscript (a, b, c, and d) indicate a statistical difference between the
 318 means, calculated using either the Student's *t* test, Welch *t* test, or Wilcoxon rank sum test. The sample size (*n*) indicates the
 319 number of plots in an NDVI data group.

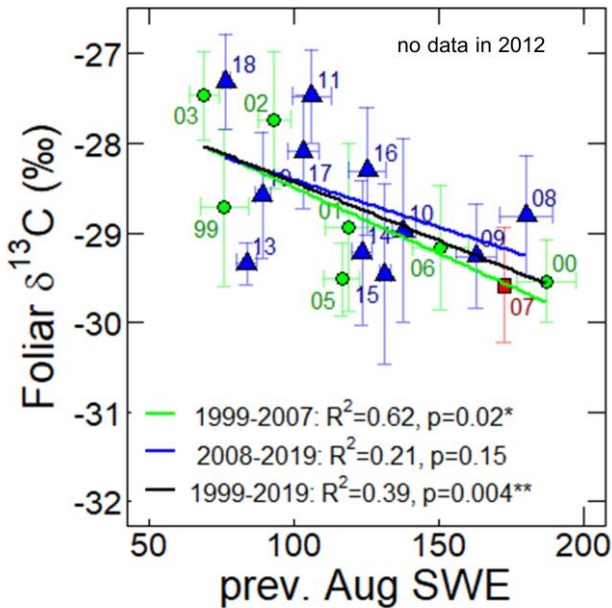
Forest type	before the wet event				
	wet period (2000–2001, 2006)	dry period (2002)	1999–2006	during the wet event (2007)	after the wet event (2008–2019)
Typical	0.78 ± 0.02^a (<i>n</i> =54)	0.73 ± 0.02^b (<i>n</i> =17)	$0.75 \pm 0.03^{c,d}$ (<i>n</i> =120)	0.76 ± 0.02^e (<i>n</i> =17)	0.75 ± 0.02^d (<i>n</i> =182)
Regenerating 1	0.79 ± 0.03^a (<i>n</i> =33)	0.73 ± 0.02^b (<i>n</i> =11)	0.76 ± 0.03^e (<i>n</i> =86)	0.72 ± 0.03^b (<i>n</i> =11)	0.74 ± 0.03^b (<i>n</i> =115)

320 3.3.4 Larch needle $\delta^{13}\text{C}$, $\delta^{15}\text{N}$, C/N at the typical forest

321 As shown in Fig. 3a and 3d, the foliar $\delta^{13}\text{C}$ and TF NDVI moved in opposite directions in the early half of the observation
 322 period (from 1999 to 2009) (Fig. 3a and 3d). For example, in 2000 and 2001, the TF NDVI had large values, while the foliar
 323 $\delta^{13}\text{C}$ values were low (-29.5 ± 0.5 and $-28.9 \pm 0.9\text{‰}$). During the period from 2002 to 2007, TF NDVI increased, and at the
 324 same time, foliar $\delta^{13}\text{C}$ values decreased. Foliar $\delta^{13}\text{C}$ values higher than -28.0‰ were observed in 2002, 2003, 2011, and
 325 2018, when low summer SWE and TF NDVI were observed (Fig. 3a and 3d). The correlation between foliar $\delta^{13}\text{C}$ and TF
 326 NDVI was statistically insignificant without a time lag (Fig. 3e, Tables S5–7), but there was a significant correlation between
 327 foliar $\delta^{13}\text{C}$ and TF NDVI with a one-year time lag of foliar $\delta^{13}\text{C}$ after the wet event (Table S6). Foliar $\delta^{13}\text{C}$ was negatively
 328 correlated with the previous August SWE during 1999–2007 ($r = -0.79$, $p < 0.05$) and 1999–2019 ($r = -0.62$, $p < 0.01$ (Fig.
 329 5), but also with the SWE in the current year June and July for the period from 1999 to 2007, and June to August for 2008 to
 330 2019 (Table S8).

331 Similar to $\delta^{13}\text{C}$, foliar C/N and TF NDVI moved in opposite directions (Fig. 3a and 3f). In 2000 and 2001, the foliar C/N had
 332 low values (25.6 ± 1.1 and 28.8 ± 3.4 , respectively), while the TF NDVI was high. There was also a distinct negative
 333 correlation between trends in C/N and TF NDVI before and after 2007, excluding 2019 (Fig. 4f).

334 Foliar $\delta^{15}\text{N}$ values decreased after 2005 (Figure 3e). A positive correlation was observed between foliar $\delta^{15}\text{N}$ and TF NDVI
 335 before 2007 (Fig. 3a, 3f, and 4g).



336

337 **Figure 5.** The relationship between the foliar $\delta^{13}\text{C}$ and monthly mean SWE in the previous August (mm) during 1999–2019. The green
 338 circles, red square, and blue triangles show data points during 1999–2006, 2007, and 2008–2019, respectively. Labels nearby the data
 339 points are observation years of the foliar $\delta^{13}\text{C}$. Vertical error bars represent standard deviations. The linear regressions for 1999–2007,
 340 2008–2019, and 1999–2019 are presented by green, blue, and black solid lines. p -values and R^2 describe the significance and coefficient of
 341 ion of the regression models, respectively.

342

4 Discussion

343

4.1 NDVI variation among forest conditions

344

345 Before 2007, there was a small difference in the NDVI among the four forest types (Fig. 2b and Table S3 and S4). In most
 346 some years before 2007, the NDVI values in RF and DF were higher than those in TF. The difference in elevation between
 347 the south and north ends of the transect (approximately 5 m according to Google Earth) may lead to differences in soil
 348 moisture; therefore, the RF and DF plots showed higher soil moisture contents and a lower possibility of drought compared
 349 with TF before 2007. During 2007–2008, there was a large difference in NDVI among the forest types, especially between
 350 the TF and DF (Fig. 2a). During this period, the SWE reached extremely high values (Fig. 3c), caused by a large precipitation
 351 amount during 2005–2008 (Fig. 2d). Consequently, the forest floor was partially waterlogged, resulting in damage to the
 352 larch forest, especially in the DF and RF plots. These data indicate that during the drought years (before 2007), wet sites such
 353 as DF and RF showed higher NDVI values than dry TF sites because of higher water availability. However, after 2007, the
 354 TF, which was visually unaffected by the wet event, showed a higher NDVI than the DF and RF. The presence of surface
 355 water in DF and soil saturated with water in DF and RF could also reduce the NDVI values. Water predominantly absorbs
 NIR radiation and therefore has a low NIR reflectance, resulting in a lower NDVI than that of vegetation (Holben, 1986).

356 After 2009, as the soil became dry, the difference in NDVI among the forest types decreased (Fig. 2b). This may have been
357 caused by the change in the vegetation in RF and DF, that is, the change from mature larch trees to understory and floor
358 vegetation, such as water-tolerant species and seedlings of birch and larch trees via secondary succession. In 2016, the
359 difference in NDVI between TF and DF increased again (Fig. 2b). This may have been caused by the high SWE observed in
360 2015 (Fig. 3c), which lowered the NDVI in RF and DF.

361 However, the difference in NDVI between TF and DF remained at the end of the observation period. Previously, the spatial
362 variation in NDVI along the transect was investigated a decade after the wet event in 2018 (Nogovitcyn et al., 2022).
363 Nogovitcyn et al. (2022) concluded that NDVI was higher in TF than in DF because of a difference in the stand density of
364 mature trees, as NDVI indicates a leaf area index (LAI), which corresponds to the number of mature trees in this forest.

365 As described in the Methods 2.2, we combined images from three Landsat satellites with different sensors. Although
366 combining data from different sensors can lead to uncertainty in the signals (Shin et al., 2023), our result or historical
367 variation in the NDVI reflected the change in the forest condition observed *in situ*.

368 4.2 Trends in NDVI of the transect and 10-km plot

369 The NDVI of the 10-km plot showed a trend similar to that of the transect NDVI during the observation period ($r = 0.78, p <$
370 0.001), as shown in Fig. 2a, and the mean NDVI value of the 10-km plot was lower than that of the transect in most years.
371 We found year-to-year variations in both NDVI datasets, but no significant increasing or decreasing trends were observed,
372 which is consistent with the observations during previous studies at this site (Nagano et al., 2022; Tei et al., 2019b; Lloyd et
373 al., 2011). Therefore, our observational data can be used for the analyses of ecosystem changes not only at the plot scale but
374 also at the regional scale.

375 4.3 Historical variation in NDVI of typical forest

376 We studied historical variations in NDVI and field-observed ecosystem and climatic parameters of a typical forest to
377 understand forest conditions.

378 4.3.1 Water availability

379 As described in the Sect. 3.3.3, SWE controls forest NDVI because the observation site (northeastern taiga) is established in
380 a continental dry area. We found positive and negative correlations between the NDVI and SWE. Before 2007, the TF NDVI
381 was positively correlated with the June SWE in the current year (Fig. 4b) and positively correlated with the SWE in the
382 previous year June, July, August, and the previous year summer (JJA: June–July–August) (Fig. 4c, 4d, S4c, and S4d, Table
383 S5). This indicates the influence of hydrological conditions in the previous year and early summer of the current year on the
384 leaf productivity of larch trees in the current year.

385 Larches, as deciduous trees, assimilate carbon through photosynthesis (photoassimilate) during the summer to prepare
386 needles in the next year, and the elongation of needles may be affected by hydrological conditions in the early summer. In the
387 Spasskaya Pad Forest, pulse-labeling experiments with $^{13}\text{CO}_2$ showed that stored carbon from the previous year contributed
388 approximately 50 % to formation of new needles in *Larix gmelini* saplings (Kagawa et al., 2006). The high level of water
389 availability in the summers of 1999 and 2000 **likely** contributed to increased carbon storage and, as a result, the high
390 formation of needles in 2000 and 2001. The significant NDVI decrease in 2002 was **probably** caused by a low level of soil
391 moisture (i.e., dry conditions). The high summer air temperature (Fig. 2c) and the small amount of precipitation (Fig. 2d) in
392 2001 and 2002 caused droughts in 2002 and 2003. Subsequently, the soil moisture increased due to a large amount of water
393 year precipitation (Fig. 2d), which **likely** contributed to an increase in NDVI until 2007.

394 It is known that the NDVI depends on the previous-year precipitation in arid and semi-arid regions (e.g., Burry et al., 2018;
395 Camberlin et al., 2007). In addition, historical time series of climate indices, based on both precipitation and temperature,
396 were related to one-year lagged NDVI (e.g., Verbyla, 2015; Liu et al., 2017). In boreal interior Alaska, the summer moisture
397 index showed a correlation with maximum summer NDVI not only at a one-year time lag in two 10-km climate station
398 buffers but also at a two-year time lag in many other ones (Verbyla, 2015). Possible reasons for the multi-year NDVI lag
399 could be the long-term negative vegetation responses to drought events, such as a decrease in carbon allocation by plants
400 (e.g., Kannenberg et al., 2019) and plant mortality (e.g., Anderegg et al., 2012). Negative effects of drought events also
401 occurred in our study.

402 ~~The effect of the preceding hydrological conditions on NDVI is also evidenced by the significant negative correlation
403 between foliar $\delta^{13}\text{C}$ and the previous August SWE during 1999–2007 ($r = -0.79, p < 0.05$; Fig. 5). The mechanism by which
404 plant $\delta^{13}\text{C}$ responds to changes in light and water availability has been well explained in previous studies (e.g., Farquhar et
405 al., 1989). Under drought stress during 2001–2002, there was a decrease in needle stomatal conductance, resulting in a
406 decrease in carbon assimilation. In the subsequent years, 2002–2003, larches produced fewer needles (lower NDVI) from the
407 previously photosynthesized carbon, and as a result, had high $\delta^{13}\text{C}$ values. Comparing the decrease in TF NDVI for drought
408 events, the decrease in TF NDVI for the extreme wet event was not as large (Fig. 2b and 3a), although the extreme wet event
409 caused a significant decrease in the NDVI of RF 1 and RF 2. However, As described above, the positive correlations between
410 the TF NDVI and soil moisture were observed during 1999–2006; however, the correlations were shifted to negative values
411 during 2008–2019 (Fig. 4b–d and S4a–e). After 2007, the TF NDVI was negatively correlated with the SWE of all months in
412 the previous (with a one-year time lag) and current years (without a lag) (Table S6). This may indicate that after the extreme
413 wet event, the soil moisture in the previous and current years seemed to negatively affect the current TF NDVI. Therefore, a
414 high level of soil moisture may affect needle production (i.e., carbon assimilation, needle formation, and/or needle
415 elongation).~~

416 Additionally, the $\delta^{13}\text{C}$ values of needles at our study site often depend on water availability (Kagawa et al., 2003; Tei et al.,
417 2019a). As shown in Fig. 5, there was the significant negative correlation between foliar $\delta^{13}\text{C}$ and the previous August SWE
418 in 1999–2007 ($r = -0.79$, $p < 0.05$). Interestingly, not only before the wet event but also for the whole observation period
419 (1999–2019), a negative correlation was found between foliar $\delta^{13}\text{C}$ and the previous August SWE (Fig. 5). These results
420 differed from the correlations between the NDVI and SWE, which changed from positive to negative values. Before the wet
421 event, under drought stress during 2001–2002, needle stomatal conductance was decreased, resulting in decreased carbon
422 assimilation. In the subsequent years, 2002–2003, larches probably produced fewer needles (lower NDVI) with higher $\delta^{13}\text{C}$
423 from the previously photosynthesized C (Fig. 3a and 3d).

424 ~~However, based on the foliar $\delta^{13}\text{C}$ data, there was no evidence that the needle stomatal conductance, which is an indicator of
425 the rates of transpiration and carbon assimilation, was disturbed by the event because the correlation between~~ After the wet
426 event, the foliar $\delta^{13}\text{C}$ and SWE remained negative, indicating high stomatal conductance (low foliar $\delta^{13}\text{C}$). During 2008–
427 2019, foliar $\delta^{13}\text{C}$ was mainly controlled by hydrological conditions in the current year rather than those in the previous year.
428 ~~In years with a high SWE, such as 2009 and 2015, stomatal conductance increased (low foliar $\delta^{13}\text{C}$), which usually indicates~~
429 High stomatal conductance typically contributes to the higher potential of a plant to assimilate CO_2 , store C, and produce
430 needles (high TF NDVI); however, after the wet period, larch produced fewer needles (low TF NDVI).

431 Compared with the decrease in the TF NDVI for drought events, that for the extreme wet event was smaller (Fig. 2b and 3a),
432 although the extreme wet event caused a significant decrease in the NDVI of RF-1 and RF-2. The decrease in the TF NDVI
433 in wet years may be due to different factors, such as nitrogen availability for larches, which can control needle formation.
434 This factor will be discussed in the next chapter.

435 4.3.2 Nitrogen availability

436 Before 2007, the TF NDVI showed a significant negative correlation with foliar C/N (Fig. 4f), indicating a positive
437 correlation with foliar N content. In this ecosystem, there have been no previous studies on the temporal correlation between
438 NDVI and plant N content (or $\delta^{15}\text{N}$). Changes in leaf nitrogen, which is an important element of chlorophyll (green pigment),
439 were detected using NDVI (Gamon et al., 1995). Previously, the relationship between NDVI and leaf N content was
440 predominantly investigated in crops for agricultural purposes but not in natural ecosystems. In coniferous forests, the
441 estimation of foliar nitrogen using remote-sensing methods showed the highest uncertainty due to the complex structure of
442 needleleaf canopies (reviewed by Homolova et al., 2013).

443 As leaf N content is considered to be an indicator of nitrogen availability for a plant in some boreal regions, where the
444 ecosystem is usually poor in N (Matsushima et al., 2012; Liang et al., 2014), we concluded that forest greenness (NDVI) was
445 strongly controlled by nitrogen uptake by larch trees. Therefore, soil moisture is suggested to play a crucial role in
446 maintaining forest nitrogen status. During 2000–2001, soil water was available for plants and induced favorable conditions

447 for soil nitrogen uptake by trees. Under suitable soil moisture conditions, the production of soil inorganic N may increase.
448 This may lead to a high production of larch needles (high NDVI). During 2002–2003—the drought years—dry conditions
449 caused less productivity of soil inorganic N and less N uptake by trees. In the post-drought period of 2004–2007, an increase
450 in soil moisture gradually recovered the forest conditions in terms of nitrogen uptake and needle production.

451 After 2007, the foliar C/N still showed a negative correlation with the TF NDVI during 2008–2018, but this correlation was
452 statistically weaker compared to that during 1999–2006 (Fig. 4f). At the same time, the positive correlations between the TF
453 NDVI and SWE changed to negative ones during 2008–2019. According to these results, high soil moisture could lead to low
454 needle production under low nitrogen availability. When extremely high soil moisture, resulting in the saturation of soil with
455 water, caused less production of soil inorganic nitrogen, low TF NDVI and high C/N values may be observed; thus, TF NDVI
456 and SWE were negatively correlated.

457 While N content reflects the plant's nitrogen status, plant $\delta^{15}\text{N}$ is widely accepted to depend on the isotopic composition of
458 nitrogen sources (e.g., Evans, 2001). Therefore, the $\delta^{15}\text{N}$ of soil inorganic ammonium NH_4^+ , which is the main nitrogen
459 source in the Spasskaya Pad forest (Popova et al., 2013), presumably determined the foliar $\delta^{15}\text{N}$ in larches. As shown in Fig.
460 3e, foliar $\delta^{15}\text{N}$ gradually decreased after 2005. These data suggest that larch trees used less soil inorganic N, especially from
461 the deeper soil layers, which usually have higher soil $\delta^{15}\text{N}$ (Amundson et al., 2003; Fujiyoshi et al., 2017). This may be
462 related to either a change in soil N dynamics, a decrease in the vertical distribution of roots (Takenaka et al., 2016), or
463 damage to the lower roots due to extremely high soil moisture. Under root oxygen stress due to soil flooding, plant
464 metabolism changes from aerobic respiration to anaerobic fermentation, characterized by energy deficiency and ethanol
465 production, both of which induce decreased nutrient uptake and plant growth (reviewed by Pezeshki and Delaune, 2012).
466 Reduced soil conditions can also induce soil phytotoxin production, damaging the root system (Pezeshki, 2001).

467 It should be noted that not only the extreme wet event in 2007, but also the extreme drought in 2001 may have caused a
468 change in N availability. Many studies have shown that foliar $\delta^{15}\text{N}$ increases during drought (Penuelas et al., 2000; Handley
469 et al., 1999; Lopes and Araus, 2006; Ogaya and Penuelas, 2008). However, in the present study, the drought in 2001 and
470 2002 decreased foliar $\delta^{15}\text{N}$. We could not identify the exact reason, but drought in 2001 and 2002 might have affected the N
471 availability for larch trees.

472 4.3.3 NDVI and RWI of larch trees

473 Two parameters of aboveground biomass, the RWI and TF NDVI, were positively correlated at a significant level ($r = 0.76$, p
474 < 0.05 ; Fig. 4a) during 1999–2006. Similarly, in other northern regions, temporal patterns of the NDVI and
475 dendrochronological data were similar for larch (Erasmi et al., 2021; Berner et al., 2011; Berner et al., 2013), pine (Berner et
476 al., 2011), and spruce (Andreu-Hayles et al., 2011; Beck et al., 2013; Berner et al., 2011; Lopatin et al., 2006). This means
477 that tree growth (RWI) and needle production (NDVI as an indicator of LAI) showed synchronous responses to

478 environmental changes before 2007. However, there was no significant correlation between the TF NDVI and RWI after
479 2007. Thus, the extreme wet event in 2007 could have changed the physiological response of larch trees to the environment
480 in terms of needle and wood production.

481 The correlation between NDVI and RWI at our observation site was previously reported by Tei et al. (2019b). They used
482 GIMMS-NDVI3g and found its positive correlation with the RWI in the subsequent year during 2004–2014 at the study site.
483 These two parameters, the NDVI and RWI, reflect the carry-over of carbon, which is fixed via needles in the previous year
484 and used in the current year, as experimentally demonstrated by Kagawa et al. (2006). ~~In our study, we could not find a~~
485 ~~significant correlation between the TF NDVI and RWI at the one-year lag of RWI (Fig. S4g).~~ In previous studies,
486 dendrochronological data showed that tree growth responded to climate with a time lag (e.g., Tei and Sugimoto, 2018). ~~In our~~
487 ~~study, we did not observe a significant correlation between the TF NDVI and RWI at the one-year lag of RWI (Fig. S4g).~~ ~~In~~
488 ~~our study, soil moisture and nitrogen availability for trees seemed to be the key factors of the environment affecting not only~~
489 ~~the NDVI, as mentioned above, but also the RWI. However, the TF NDVI and RWI were not significantly correlated after~~
490 ~~2007, whereas there was a significant positive correlation before 2007. Thus, the extreme wet event in 2007 could have~~
491 ~~changed the physiological response of larch trees to the environment in terms of needle and wood production.~~

492 4.4 Changes in larch forest NDVI due to drought and the extreme wet event

493 As shown in Fig. 2b, the NDVI in TF showed a significant decrease in 2002. Such a decrease in NDVI has been repeated in
494 the past because the climate is continental (dry) in this region. Compared to this decrease in NDVI due to drought, the
495 extreme wet event in 2007 showed only a slight decrease in the NDVI in TF, although the NDVI in DF and RF-2 decreased
496 considerably.

497 Tree mortality in the DF and RF during the extreme wet event is controlled by soil properties and topographic features, that
498 is, depressions (Iwasaki et al., 2010). However, the effects of the event may not only include tree mortality but also invisible
499 damage to living trees. In this study, NDVI, a potential indicator of needle production in a typical forest, was negatively
500 related to the summer SWE in the previous and current years during 2008–2019 and with the current-year needle C/N during
501 2008–2018 (Table S6). This may indicate that needle production in the current and subsequent years during the summer was
502 disturbed by increased soil moisture and decreased soil N uptake by trees. We suggest that N uptake by larches might be
503 reduced in wet soils due to damaged lower roots, decreased vertical distribution of roots (Takenaka et al., 2016), or altered
504 soil N production.

505 Changes in the process of needle production may affect tree growth in the current and subsequent years in the forest (Kagawa
506 et al., 2006; Tei et al., 2019b). However, we found no evidence that tree radial growth was disturbed after 2007, and the RWI
507 responded well to changes in the SWE (Fig. 3b and 3c). Additionally, at the ecosystem scale, there was no significant change
508 in the CO₂ exchange measured by the 32-m flux tower in this larch forest (Kotani et al., 2019). However, the observed

509 increase in understory biomass was suggested to compensate for negative changes in fluxes at the overstory level (Kotani et
510 al., 2019) and in the NDVI of the forest (Nagano et al., 2022). This means that the negative effects of the extreme wet event
511 on living larch trees were not excluded in the previous studies. Our study showed that limitation in N uptake at high soil
512 moisture levels is one of the factors that may potentially reduce tree growth in the future.

513 In our previous study (Nogovitcyn et al., 2022), spatial variations in NDVI and foliar traits identified favorable conditions in
514 the sites affected by the extreme wet event (RF). The larch forest in RF with lower NDVI (lower stand density) had higher
515 light (higher $\delta^{13}\text{C}$) and nitrogen (lower foliar C/N) availability for one mature larch tree than that in unaffected areas (TF)
516 because of reduced competition for light and soil nitrogen among trees. Such favorable conditions and the presence of a large
517 number of young larch trees may lead to further RF succession after an extremely wet event. However, because weather
518 extremes are expected to be more frequent and intensive (Douville et al., 2021), the period between extremes may exceed the
519 period of recovery after the extremes. Therefore, in the future, forests may be damaged rather than recovered.

520 We showed that NDVI values in affected areas were lower than those in typical larch forests for more than 10 years after the
521 extreme wet event. In other boreal regions, the NDVI was higher in damaged forests because of the strong contribution of
522 understory to surface greenness (Bunn et al., 2007; Dearborn and Baltzer, 2021), suggesting the need to combine field and
523 remote sensing observations. Regarding the prediction of tree growth in this dry region, there is a discrepancy between the
524 different vegetation models. The dynamic global vegetation model (DGVM) simulated increased forest production
525 throughout the circumboreal region in the nearest century, whereas the RWI-based model showed the opposite result in the
526 regions of Alaska, Canada, Europe and our study site (Tei et al., 2017). In these regions with a continentally dry climate, tree
527 growths suffers because of the effects of temperature-induced drought stress and are predicted to decrease under warming
528 conditions (Tei et al., 2017). In addition, extreme wet events are also likely to have a negative impact on forest production
529 because of changes in nitrogen availability, as demonstrated in this study. Some models may overestimate production
530 because they do not include important parameters such as soil moisture, soil N production, and N uptake by trees. To better
531 understand changes in the forest, long-term observation of variations in soil N availability depending on soil moisture and
532 other factors is necessary.

533 5 Conclusions

534 In this study, historical variations in satellite-derived NDVI (**seasonal maximum**) and field-observed parameters of larch
535 forests were investigated to understand the effects of the extreme wet event on the larch forests of northeastern Siberia. The
536 NDVI values of the plots visually unaffected (typical mature larch forest, TF) and affected by the event were similar before
537 2007, and the NDVI values at both plots were similarly decreased by drought. However, both NDVI values ~~but~~ differed after
538 2007 because of the high tree mortality in affected plots caused by waterlogging and the presence of water in the depression.

539 Although the TF was visually unaffected by the event, it also changed. Before the wet event, the positive relationship
540 between the TF NDVI and SWE in the previous summer and the current June showed that needle production increased with
541 water availability, as previously observed in this dry region. However, after the wet event, the relationship between the TF
542 NDVI and soil moisture in the previous and current years unexpectedly shifted from positive to negative, which may have
543 been related to N availability. ~~Temporal correlations revealed that before the wet event, needle production (TF NDVI) was~~
544 ~~positively related to the SWE in the previous summer and current June and tree ring growth (RWI). In this dry region,~~
545 ~~larches used the previous year soil water to make photosynthates (carbon assimilated by photosynthesis) to prepare needles~~
546 ~~and wood in the current year and used the early summer soil water for the elongation of needles in the current year.~~

547 N is considered an important factor controlling needle production before and after the wet event, as the negative correlations
548 between TF NDVI and needle C/N ratio were observed until 2018 (except for in 2007). In addition, the needle $\delta^{15}\text{N}$
549 continuously decreased after the wet event, suggesting that the larch trees used a different N source when the lower roots
550 were damaged by anaerobic conditions. Before the wet event, the high (but suitable) soil moisture level presumably produced
551 more soil inorganic N, and consequently produced more larch needles, whereas the extreme wetness after 2007 likely had a
552 long-term negative effect on needle production because of the lower soil N production. As shown in this study, extreme wet
553 events in continental dry regions may alter the interaction between water availability and tree performance (for example,
554 NDVI) over a long time because of shifts in N availability for trees.

555 ~~In addition, the TF NDVI showed significant negative correlations with needle C/N ratio (or positive correlation with needle~~
556 ~~N content) before the wet event, and this correlation continued until 2018 (except for 2007). This indicates that nitrogen is an~~
557 ~~important parameter for this ecosystem before and after a wet event. The $\delta^{15}\text{N}$ in 1999–2006 showed a positive correlation~~
558 ~~with TF NDVI. Under suitable soil moisture conditions, the production of soil inorganic N, and consequently, the production~~
559 ~~of larch needles, may be increased. However, after the wet event in 2008–2019, the temporal correlations between the TF~~
560 ~~NDVI and SWE in the previous summer and current June surprisingly shifted from positive to negative. Needle N content~~
561 ~~was positively correlated with the TF NDVI and negatively correlated with the SWE in June. In addition, needle $\delta^{15}\text{N}$~~
562 ~~generally decreased, indicating that larches used less inorganic nitrogen from deeper soils, which usually have higher $\delta^{15}\text{N}$.~~
563 ~~During this period, extremely high soil moisture may have caused inactive soil inorganic N, anaerobic stress induced root~~
564 ~~damage, and/or production of soil phytotoxins, which decreased nitrogen uptake and plant growth.~~

565 **Data availability.** Yakutsk air temperature and precipitation data are available from the RIHMI-WDC website (<http://aisori-m.meteo.ru/>). NDVI data was calculated from Landsat 5, 7, 8 images, which are available from the USGS website
566 (<https://earthexplorer.usgs.gov/>). The seasonal maximum NDVI data and larch RWI data are described in the Supplement
567 (Table S1 and S2). All other data presented in this work have been deposited in the Arctic Data Archive System (ADS): **soil**

569 moisture data at Spasskaya Pad (<https://ads.nipr.ac.jp/dataset/A20230217-001>) and larch needle C/N and carbon and nitrogen
570 isotopes at Spasskaya Pad (<https://ads.nipr.ac.jp/dataset/A20230217-002>).

571 **Author contributions.** AS designed the research and AN calculated the NDVI and performed the analyses. TM, ST, and NS
572 helped with the analyses, and TCM managed all the field observations. RS and YM helped with field observations. AN and
573 AS prepared the paper with contributions from all co-authors.

574 **Competing interests.** The authors declare that they have no conflict of interest.

575 **Acknowledgements.** The authors are grateful to Dr. A. Kononov, R. Petrov, and other colleagues from the IBPC for
576 supporting our fieldwork at the Spasskaya Pad Forest Station and M. Grigorev for his assistance in the fieldwork. The
577 authors also appreciate Y. Hoshino, S. Nunohashi, A. Alekseeva, and E. Starostin for their support in laboratory work and
578 logistics.

579 **Financial support.** This work was supported by the Belmont Forum Arctic program COPERA (C budget of ecosystems,
580 cities, and villages on permafrost in the eastern Russian Arctic) project, the International Priority Graduate Programs (IPGP),
581 funded by the Ministry of Education, Culture, Sports, Science, and Technology-Japan (MEXT), and the Hokkaido University
582 DX Doctoral Fellowship (Grant No. JPMJSP2119), funded by the Japan Science and Technology Agency.

583 **References**

584 Abaimov, A. P., Lesinski, J. A., Martinsson, O., and Milyutin, L. I.: Variability and ecology of Siberian larch species,
585 Swedish University of Agricultural Sciences. Departament of Silviculture. Reports., Umeå, 123 pp., 1998.

586 Amundson, R., Austin, A. T., Schuur, E. A. G., Yoo, K., Matzek, V., Kendall, C., Uebersax, A., Brenner, D., and Baisden, W.
587 T.: Global patterns of the isotopic composition of soil and plant nitrogen, *Global Biogeochemical Cycles*, 17,
588 10.1029/2002gb001903, 2003.

589 Anderegg, W. R. L., Berry, J. A., Smith, D. D., Sperry, J. S., Anderegg, L. D. L., and Field, C. B.: The roles of hydraulic and
590 carbon stress in a widespread climate-induced forest die-off, *Proceedings of the National Academy of Sciences of the United
591 States of America*, 109, 233-237, 10.1073/pnas.1107891109, 2012.

592 Andreu-Hayles, L., D'Arrigo, R., Anchukaitis, K. J., Beck, P. S. A., Frank, D., and Goetz, S.: Varying boreal forest response
593 to Arctic environmental change at the Firth River, Alaska, *Environmental Research Letters*, 6, 10.1088/1748-
594 9326/6/4/045503, 2011.

595 Archibald, O. W.: The coniferous forests, in: *Ecology of World Vegetation*, 238–279, 10.1007/978-94-011-0009-0_8 1995.

596 Beck, P. S. A., Andreu-Hayles, L., D'Arrigo, R., Anchukaitis, K. J., Tucker, C. J., Pinzon, J. E., and Goetz, S. J.: A large-scale
597 coherent signal of canopy status in maximum latewood density of tree rings at arctic treeline in North America, *Global and*

598 Planetary Change, 100, 109-118, 10.1016/j.gloplacha.2012.10.005, 2013.

599 Berner, L. T., Beck, P. S. A., Bunn, A. G., and Goetz, S. J.: Plant response to climate change along the forest-tundra ecotone
600 in northeastern Siberia, Global Change Biology, 19, 3449-3462, 10.1111/gcb.12304, 2013.

601 Berner, L. T., Beck, P. S. A., Bunn, A. G., Lloyd, A. H., and Goetz, S. J.: High-latitude tree growth and satellite vegetation
602 indices: Correlations and trends in Russia and Canada (1982-2008), Journal of Geophysical Research-Biogeosciences, 116,
603 10.1029/2010jg001475, 2011.

604 Bunn, A. G. and Goetz, S. J.: Trends in satellite-observed circumpolar photosynthetic activity from 1982 to 2003: The
605 influence of seasonality, cover type, and vegetation density, Earth Interactions, 10, 2006.

606 Bunn, A. G., Goetz, S. J., Kimball, J. S., and Zhang, K.: Northern high-latitude ecosystems respond to climate change,
607 10.1029/2007EO340001, 2007.

608 Burry, L. S., Palacio, P. I., Somoza, M., de Mandri, M. E. T., Lindskoug, H. B., Marconetto, M. B., and D'Antoni, H. L.:
609 Dynamics of fire, precipitation, vegetation and NDVI in dry forest environments in NW Argentina. Contributions to
610 environmental archaeology, Journal of Archaeological Science-Reports, 18, 747-757, 10.1016/j.jasrep.2017.05.019, 2018.

611 Camberlin, P., Martiny, N., Philippon, N., and Richard, Y.: Determinants of the interannual relationships between remote
612 sensed photosynthetic activity and rainfall in tropical Africa, Remote Sensing of Environment, 106, 199-216,
613 10.1016/j.rse.2006.08.009, 2007.

614 Dearborn, K. D. and Baltzer, J. L.: Unexpected greening in a boreal permafrost peatland undergoing forest loss is partially
615 attributable to tree species turnover, Global Change Biology, 27, 2867-2882, 10.1111/gcb.15608, 2021.

616 Douville, H., Raghavan, K., Renwick, J., Allan, R. P., Arias, P. A., Barlow, M., Cerezo-Mota, R., Cherchi, A., Gan, T. Y.,
617 Gergis, J., Jiang, D., Khan, A., Pokam Mba, W., Rosenfeld, D., Tierney, J., and Zolina, O.: Water Cycle Changes, in: Climate
618 Change 2021: The Physical Science Basis. Contribution of Working Group I to the Sixth Assessment Report of the
619 Intergovernmental Panel on Climate Change edited by: Masson-Delmotte, V., Zhai, P., Pirani, A., Connors, S. L., Péan, C.,
620 Berger, S., Caud, N., Chen, Y., Goldfarb, L., Gomis, M. I., Huang, M., Leitzell, K., Lonnoy, E., Matthews, J. B. R., Maycock,
621 T. K., Waterfield, T., Yelekçi, O., Yu, R., and Zhou, B., Cambridge University Press, Cambridge, United Kingdom and New
622 York 1055-1210, 10.1017/9781009157896.010.—, 2021.

623 Erasmi, S., Klinge, M., Dulamsuren, C., Schneider, F., and Hauck, M.: Modelling the productivity of Siberian larch forests
624 from Landsat NDVI time series in fragmented forest stands of the Mongolian forest-steppe, Environmental Monitoring and
625 Assessment, 193, 10.1007/s10661-021-08996-1, 2021.

626 Evans, R. D.: Physiological mechanisms influencing plant nitrogen isotope composition, Trends in Plant Science, 6, 121-126,
627 10.1016/s1360-1385(01)01889-1, 2001.

628 Famiglietti, C. A., Michalak, A. M., and Konings, A. G.: Extreme wet events as important as extreme dry events in
629 controlling spatial patterns of vegetation greenness anomalies, Environmental Research Letters, 16, 10.1088/1748-
630 9326/abfc78, 2021.

631 Fan, R., Shimada, H., Tei, S., Maximov, T. C., and Sugimoto, A.: Oxygen Isotope Compositions of Cellulose in Earlywood of
632 Larix cajanderi Determined by Water Source Rather Than Leaf Water Enrichment in a Permafrost Ecosystem, Eastern
633 Siberia, Journal of Geophysical Research-Biogeosciences, 126, 10.1029/2020jg006125, 2021.

634 FAO: Global Forest Resources Assessment 2020 – Key findings, Rome, 10.4060/ca8753en, 2020.

635 Farquhar, G. D., Ehleringer, J. R., and Hubick, K. T.: Carbon isotope discrimination and photosynthesis, Annual Review of
636 Plant Physiology and Plant Molecular Biology, 40, 503-537, 10.1146/annurev.pp.40.060189.002443, 1989.

637 Forbes, B. C., Fauria, M. M., and Zetterberg, P.: Russian Arctic warming and 'greening' are closely tracked by tundra shrub
638 willows, Global Change Biology, 16, 1542-1554, 10.1111/j.1365-2486.2009.02047.x, 2010.

639 Forkel, M., Migliavacca, M., Thonicke, K., Reichstein, M., Schaphoff, S., Weber, U., and Carvalhais, N.: Codominant water
640 control on global interannual variability and trends in land surface phenology and greenness, Global Change Biology, 21,
641 3414-3435, 10.1111/gcb.12950, 2015.

642 Friedlingstein, P., Jones, M. W., O'Sullivan, M., Andrew, R. M., Bakker, D. C. E., Hauck, J., Le Quere, C., Peters, G. P.,
643 Peters, W., Pongratz, J., Sitch, S., Canadell, J. G., Ciais, P., Jackson, R. B., Alin, S. R., Anthoni, P., Bates, N. R., Becker, M.,
644 Bellouin, N., Bopp, L., Chau, T. T. T., Chevallier, F., Chini, L. P., Cronin, M., Currie, K. I., Decharme, B., Djedjchouang, L.
645 M., Dou, X. Y., Evans, W., Feely, R. A., Feng, L., Gasser, T., Gilfillan, D., Gkrizalis, T., Grassi, G., Gregor, L., Gruber, N.,
646 Gurses, O., Harris, I., Houghton, R. A., Hurtt, G. C., Iida, Y., Ilyina, T., Luijkx, I. T., Jain, A., Jones, S. D., Kato, E., Kennedy,
647 D., Goldewijk, K. K., Knauer, J., Korsbakken, J. I., Kortzinger, A., Landschutze, P., Lauvset, S. K., Lefevre, N., Lienert, S.,
648 Liu, J. J., Marland, G., McGuire, P. C., Melton, J. R., Munro, D. R., Nabel, J., Nakaoka, S. I., Niwa, Y., Ono, T., Pierrot, D.,
649 Poulter, B., Rehder, G., Resplandy, L., Robertson, E., Rodenbeck, C., Rosan, T. M., Schwinger, J., Schwingshakl, C.,
650 Seferian, R., Sutton, A. J., Sweeney, C., Tanhua, T., Tans, P. P., Tian, H. Q., Tilbrook, B., Tubiello, F., van der Werf, G. R.,
651 Vuichard, N., Wada, C., Wanminkhof, R., Watson, A. J., Willis, D., Wiltshire, A. J., Yuan, W. P., Yue, C., Yue, X., Zaehle, S.,
652 and Zeng, J. Y.: Global Carbon Budget 2021, Earth System Science Data, 14, 1917-2005, 10.5194/essd-14-1917-2022, 2022.

653 Frost, G. V. and Epstein, H. E.: Tall shrub and tree expansion in Siberian tundra ecotones since the 1960s, Global Change
654 Biology, 20, 1264-1277, 10.1111/gcb.12406, 2014.

655 Fujiyoshi, L., Sugimoto, A., Tsukuura, A., Kitayama, A., Caceres, M. L. L., Mijidsuren, B., Saraadanbazar, A., and
656 Tsujimura, M.: Spatial variations in larch needle and soil N-15 at a forest-grassland boundary in northern Mongolia, Isotopes
657 in Environmental and Health Studies, 53, 54-69, 10.1080/10256016.2016.1206093, 2017.

658 Gamon, J. A., Field, C. B., Goulden, M. L., Griffin, K. L., Hartley, A. E., Joel, G., Penuelas, J., and Valentini, R.:
659 Relationships between NDVI, canopy structure, and photosynthesis in 3 Californian vegetation types, Ecological
660 Applications, 5, 28-41, 10.2307/1942049, 1995.

661 Goetz, S. J., Bunn, A. G., Fiske, G. J., and Houghton, R. A.: Satellite-observed photosynthetic trends across boreal North
662 America associated with climate and fire disturbance, Proceedings of the National Academy of Sciences of the United States
663 of America, 102, 13521-13525, 10.1073/pnas.0506179102, 2005.

664 Handley, L. L., Azcon, R., Lozano, J. M. R., and Scrimgeour, C. M.: Plant delta N-15 associated with arbuscular
665 mycorrhization, drought and nitrogen deficiency, Rapid Communications in Mass Spectrometry, 13, 1320-1324, 1999.

666 Holben, B. N.: Characteristics of maximum-value composite images from temporal AVHRR data, International Journal of
667 Remote Sensing, 7, 1417-1434, 10.1080/01431168608948945, 1986.

668 Homolova, L., Maenovsky, Z., Clevers, J., Garcia-Santos, G., and Schaeprnan, M. E.: Review of optical-based remote
669 sensing for plant trait mapping, Ecological Complexity, 15, 1-16, 10.1016/j.ecocom.2013.06.003, 2013.

670 Huete, A., Didan, K., Miura, T., Rodriguez, E. P., Gao, X., and Ferreira, L. G.: Overview of the radiometric and biophysical
671 performance of the MODIS vegetation indices, *Remote Sensing of Environment*, 83, 195-213, 10.1016/s0034-
672 4257(02)00096-2, 2002.

673 Iijima, Y., Ohta, T., Kotani, A., Fedorov, A. N., Kodama, Y., and Maximov, T. C.: Sap flow changes in relation to permafrost
674 degradation under increasing precipitation in an eastern Siberian larch forest, *Ecohydrology*, 7, 177-187, 10.1002/eco.1366,
675 2014.

676 Iwasaki, H., Saito, H., Kuwao, K., Maximov, T. C., and Hasegawa, S.: Forest decline caused by high soil water conditions in
677 a permafrost region, *Hydrology and Earth System Sciences*, 14, 301-307, 10.5194/hess-14-301-2010, 2010.

678 Ju, J. C. and Masek, J. G.: The vegetation greenness trend in Canada and US Alaska from 1984-2012 Landsat data, *Remote
679 Sensing of Environment*, 176, 1-16, 10.1016/j.rse.2016.01.001, 2016.

680 Kagawa, A., Sugimoto, A., and Maximov, T. C.: Seasonal course of translocation, storage and remobilization of C-13 pulse-
681 labeled photoassimilate in naturally growing *Larix gmelinii* saplings, *New Phytologist*, 171, 793-804, 10.1111/j.1469-
682 8137.2006.01780.x, 2006.

683 Kagawa, A., Naito, D., Sugimoto, A., and Maximov, T. C.: Effects of spatial and temporal variability in soil moisture on
684 widths and delta C-13 values of eastern Siberian tree rings, *Journal of Geophysical Research-Atmospheres*, 108,
685 10.1029/2002jd003019, 2003.

686 Kajimoto, T., Matsuura, Y., Sofronov, M. A., Volokitina, A. V., Mori, S., Osawa, A., and Abaimov, A. P.: Above- and
687 belowground biomass and net primary productivity of a *Larix gmelinii* stand near Tura, central Siberia, *Tree Physiology*, 19,
688 815-822, 1999.

689 Kannenberg, S. A., Novick, K. A., Alexander, M. R., Maxwell, J. T., Moore, D. J. P., Phillips, R. P., and Anderegg, W. R. L.:
690 Linking drought legacy effects across scales: From leaves to tree rings to ecosystems, *Global Change Biology*, 25, 2978-
691 2992, 10.1111/gcb.14710, 2019.

692 Kotani, A., Saito, A., Kononov, A. V., Petrov, R. E., Maximov, T. C., Iijima, Y., and Ohta, T.: Impact of unusually wet
693 permafrost soil on understory vegetation and CO2 exchange in a larch forest in eastern Siberia, *Agricultural and Forest
694 Meteorology*, 265, 295-309, 10.1016/j.agrformet.2018.11.025, 2019.

695 Liang, M. C., Sugimoto, A., Tei, S., Bragin, I. V., Takano, S., Morozumi, T., Shingubara, R., Maximov, T. C., Kiyashko, S. I.,
696 Velivetskaya, T. A., and Ignatiev, A. V.: Importance of soil moisture and N availability to larch growth and distribution in the
697 Arctic taiga-tundra boundary ecosystem, northeastern Siberia, *Polar Science*, 8, 327-341, 10.1016/j.polar.2014.07.008, 2014.

698 Liu, J. X., Price, D. T., and Chen, J. A.: Nitrogen controls on ecosystem carbon sequestration: a model implementation and
699 application to Saskatchewan, Canada, *Ecological Modelling*, 186, 178-195, 10.1016/j.ecolmodel.2005.01.036, 2005.

700 Liu, S. L., Zhang, Y. Q., Cheng, F. Y., Hou, X. Y., and Zhao, S.: Response of Grassland Degradation to Drought at Different
701 Time-Scales in Qinghai Province: Spatio-Temporal Characteristics, Correlation, and Implications, *Remote Sensing*, 9,
702 10.3390/rs9121329, 2017.

703 Lloyd, A. H., Bunn, A. G., and Berner, L.: A latitudinal gradient in tree growth response to climate warming in the Siberian
704 taiga, *Global Change Biology*, 17, 1935-1945, 10.1111/j.1365-2486.2010.02360.x, 2011.

705 Lopatin, E., Kolstrom, T., and Spiecker, H.: Determination of forest growth trends in Komi Republic (northwestern Russia):

706 combination of tree-ring analysis and remote sensing data, *Boreal Environment Research*, 11, 341-353, 2006.

707 Lopes, M. S. and Araus, J. L.: Nitrogen source and water regime effects on durum wheat photosynthesis and stable carbon

708 and nitrogen isotope composition, *Physiologia Plantarum*, 126, 435-445, 10.1111/j.1399-3054.2006.00595.x, 2006.

709 Matsumoto, K., Ohta, T., Nakai, T., Kuwada, T., Daikoku, K., Iida, S., Yabuki, H., Kononov, A. V., van der Molen, M. K.,

710 Kodama, Y., Maximov, T. C., Dolman, A. J., and Hattori, S.: Responses of surface conductance to forest environments in the

711 Far East, *Agricultural and Forest Meteorology*, 148, 1926-1940, 10.1016/j.agrformet.2008.09.009, 2008.

712 Matsushima, M., Choi, W. J., and Chang, S. X.: White spruce foliar delta C-13 and delta N-15 indicate changed soil N

713 availability by understory removal and N fertilization in a 13-year-old boreal plantation, *Plant and Soil*, 361, 375-384,

714 10.1007/s11104-012-1254-z, 2012.

715 Miles, V. V. and Esau, I.: Spatial heterogeneity of greening and browning between and within bioclimatic zones in northern

716 West Siberia, *Environmental Research Letters*, 11, 10.1088/1748-9326/11/11/115002, 2016.

717 Myers-Smith, I. H., Kerby, J. T., Phoenix, G. K., Bjerke, J. W., Epstein, H. E., Assmann, J. J., John, C., Andreu-Hayles, L.,

718 Angers-Blondin, S., Beck, P. S. A., Berner, L. T., Bhatt, U. S., Bjorkman, A. D., Blok, D., Bryn, A., Christiansen, C. T.,

719 Cornelissen, J. H. C., Cunliffe, A. M., Elmendorf, S. C., Forbes, B. C., Goetz, S. J., Hollister, R. D., de Jong, R., Loranty, M.

720 M., Macias-Fauria, M., Maseyk, K., Normand, S., Olofsson, J., Parker, T. C., Parmentier, F. J. W., Post, E., Schaepman-Strub,

721 G., Stordal, F., Sullivan, P. F., Thomas, H. J. D., Tommervik, H., Trehearne, R., Tweedie, C. E., Walker, D. A., Wilming, M.,

722 and Wipf, S.: Complexity revealed in the greening of the Arctic, *Nature Climate Change*, 10, 106-117, 10.1038/s41558-019-

723 0688-1, 2020.

724 Nagano, H., Kotani, A., Mizuochi, H., Ichii, K., Kanamori, H., and Hiyama, T.: Contrasting 20-year trends in NDVI at two

725 Siberian larch forests with and without multiyear waterlogging-induced disturbances, *Environmental Research Letters*, 17,

726 10.1088/1748-9326/ac4884, 2022.

727 Nakai, T., Hiyama, T., Petrov, R. E., Kotani, A., Ohta, T., and Maximov, T. C.: Application of an open-path eddy covariance

728 methane flux measurement system to a larch forest in eastern Siberia, *Agricultural and Forest Meteorology*, 282,

729 10.1016/j.agrformet.2019.107860, 2020.

730 Nogovitcyn, A., Shakhmatov, R., Morozumi, T., Tei, S., Miyamoto, Y., Shin, N., Maximov, T. C., and Sugimoto, A.: Changes

731 in Forest Conditions in a Siberian Larch Forest Induced by an Extreme Wet Event, *Forests*, 13, 10.3390/f13081331, 2022.

732 Ogaya, R. and Penuelas, J.: Changes in leaf delta C-13 and delta N-15 for three Mediterranean tree species in relation to soil

733 water availability, *Acta Oecologica-International Journal of Ecology*, 34, 331-338, 10.1016/j.actao.2008.06.005, 2008.

734 Ohta, T., Kotani, A., Iijima, Y., Maximov, T. C., Ito, S., Hanamura, M., Kononov, A. V., and Maximov, A. P.: Effects of

735 waterlogging on water and carbon dioxide fluxes and environmental variables in a Siberian larch forest, 1998-2011,

736 *Agricultural and Forest Meteorology*, 188, 64-75, 10.1016/j.agrformet.2013.12.012, 2014.

737 Penuelas, J., Filella, I., Lloret, F., Pinol, J., and Siscart, D.: Effects of a severe drought on water and nitrogen use by *Quercus*

738 *ilex* and *Phillyrea latifolia*, *Biologia Plantarum*, 43, 47-53, 10.1023/a:1026546828466, 2000.

739 Pezeshki, S. R.: Wetland plant responses to soil flooding, *Environmental and Experimental Botany*, 46, 299-312,

740 10.1016/s0098-8472(01)00107-1, 2001.

741 Pezeshki, S. R. and DeLaune, R. D.: Soil Oxidation-Reduction in Wetlands and Its Impact on Plant Functioning,

742 10.3390/biology1020196, 2012.

743 Popova, A. S., Tokuchi, N., Ohte, N., Ueda, M. U., Osaka, K., Maximov, T. C., and Sugimoto, A.: Nitrogen availability in the
744 taiga forest ecosystem of northeastern Siberia, *Soil Science and Plant Nutrition*, 59, 427-441,
745 10.1080/00380768.2013.772495, 2013.

746 Roy, D. P., Kovalskyy, V., Zhang, H. K., Vermote, E. F., Yan, L., Kumar, S. S., and Egorov, A.: Characterization of Landsat-7
747 to Landsat-8 reflective wavelength and normalized difference vegetation index continuity, *Remote Sensing of Environment*,
748 185, 57-70, 10.1016/j.rse.2015.12.024, 2016.

749 Ruiz-Perez, G. and Vico, G.: Effects of Temperature and Water Availability on Northern European Boreal Forests, *Frontiers*
750 in Forests and Global Change

751 Sato, H. and Kobayashi, H.: Topography Controls the Abundance of Siberian Larch Forest, *Journal of Geophysical Research-
752 Biogeosciences*, 123, 106-116, 10.1002/2017jg004096, 2018.

753 Schuur, E. A. G., McGuire, A. D., Schadel, C., Grosse, G., Harden, J. W., Hayes, D. J., Hugelius, G., Koven, C. D., Kuhry, P.,
754 Lawrence, D. M., Natali, S. M., Olefeldt, D., Romanovsky, V. E., Schaefer, K., Turetsky, M. R., Treat, C. C., and Vonk, J. E.:
755 Climate change and the permafrost carbon feedback, *Nature*, 520, 171-179, 10.1038/nature14338, 2015.

756 Shakhmatov, R., Hashiguchi, S., Maximov, T. C., and Sugimoto, A.: Effects of snow manipulation on larch trees in the taiga
757 forest ecosystem in northeastern Siberia, *Progress in Earth and Planetary Science*, 9, 10.1186/s40645-021-00460-5, 2022.

758 Sugimoto, A.: Stable Isotopes of Water in Permafrost Ecosystem, in: *Water-Carbon Dynamics in Eastern Siberia. Ecological*
759 *Studies (Analysis and Synthesis)*, edited by: Ohta, T., Hiyama, T., Iijima, Y., Kotani, A., and Maximov, T., Springer,
760 Singapore, 10.1007/978-981-13-6317-7_6, 2019.

761 Shevtsova, I., Heim, B., Kruse, S., Schroder, J., Troeva, E. I., Pestryakova, L. A., Zakharov, E. S., and Herzschuh, U.: Strong
762 shrub expansion in tundra-taiga, tree infilling in taiga and stable tundra in central Chukotka (north-eastern Siberia) between
763 2000 and 2017, *Environmental Research Letters*, 15, 10.1088/1748-9326/ab9059, 2020.

764 Shin, N., Saitoh, T. M., Takeuchi, Y., Miura, T., Aiba, M., Kurokawa, H., Onoda, Y., Ichii, K., Nasahara, K. N., Suzuki, R.,
765 Nakashizuka, T., and Muraoka, H.: Review: Monitoring of land cover changes and plant phenology by remote-sensing in
766 East Asia, *Ecological Research*, 38, 111-133, 10.1111/1440-1703.12371, 2023.

767 Sugimoto, A., Yanagisawa, N., Naito, D., Fujita, N., and Maximov, T. C.: Importance of permafrost as a source of water for
768 plants in east Siberian taiga, *Ecological Research*, 17, 493-503, 10.1046/j.1440-1703.2002.00506.x, 2002.

769 Sugimoto, A., Naito, D., Yanagisawa, N., Ichiyanagi, K., Kurita, N., Kubota, J., Kotake, T., Ohata, T., Maximov, T. C., and
770 Fedorov, A. N.: Characteristics of soil moisture in permafrost observed in East Siberian taiga with stable isotopes of water,
771 *Hydrological Processes*, 17, 1073-1092, 10.1002/hyp.1180, 2003.

772 Takata, K., Patra, P. K., Kotani, A., Mori, J., Belikov, D., Ichii, K., Saeki, T., Ohta, T., Saito, K., Ueyama, M., Ito, A.,
773 Maksyutov, S., Miyazaki, S., Burke, E. J., Ganshin, A., Iijima, Y., Ise, T., Machiya, H., Maximov, T. C., Niwa, Y., O'Ishi, R.,
774 Park, H., Sasai, T., Sato, H., Tei, S., Zhuravlev, R., Machida, T., Sugimoto, A., and Aoki, S.: Reconciliation of top-down and
775 bottom-up CO₂ fluxes in Siberian larch forest, *Environmental Research Letters*, 12, 10.1088/1748-9326/aa926d, 2017.

776 Takenaka, C., Miyahara, M., Ohta, T., and Maximov, T. C.: Response of larch root development to annual changes of water
777 conditions in eastern Siberia, *Polar Science*, 10, 160-166, 10.1016/j.polar.2016.04.012, 2016.

778 Tape, K., Sturm, M., and Racine, C.: The evidence for shrub expansion in Northern Alaska and the Pan-Arctic, *Global*
779 *Change Biology*, 12, 686-702, 10.1111/j.1365-2486.2006.01128.x, 2006.

780 Tei, S. and Sugimoto, A.: Time lag and negative responses of forest greenness and tree growth to warming over circumboreal
781 forests, *Global Change Biology*, 24, 4225-4237, 10.1111/gcb.14135, 2018.

782 Tei, S., Sugimoto, A., Yonenobu, H., Kotani, A., and Maximov, T. C.: Effects of extreme drought and wet events for tree
783 mortality: Insights from tree-ring width and carbon isotope ratio in a Siberian larch forest, *Ecohydrology*, 12,
784 10.1002/eco.2143, 2019a.

785 Tei, S., Sugimoto, A., Yonenobu, H., Yamazaki, T., and Maximov, T. C.: Reconstruction of soil moisture for the past 100
786 years in eastern Siberia by using delta C-13 of larch tree rings, *Journal of Geophysical Research-Biogeosciences*, 118, 1256-
787 1265, 10.1002/jgrg.20110, 2013.

788 Tei, S., Sugimoto, A., Kotani, A., Ohta, T., Morozumi, T., Saito, S., Hashiguchi, S., and Maximov, T.: Strong and stable
789 relationships between tree-ring parameters and forest-level carbon fluxes in a Siberian larch forest, *Polar Science*, 21, 146-
790 157, 10.1016/j.polar.2019.02.001, 2019b.

791 Tei, S., Sugimoto, A., Yonenobu, H., Matsuura, Y., Osawa, A., Sato, H., Fujinuma, J., and Maximov, T.: Tree-ring analysis
792 and modeling approaches yield contrary response of circumboreal forest productivity to climate change, *Global Change
793 Biology*, 23, 5179-5188, 10.1111/gcb.13780, 2017.

794 Verbyla, D.: The greening and browning of Alaska based on 1982-2003 satellite data, *Global Ecology and Biogeography*, 17,
795 547-555, 10.1111/j.1466-8238.2008.00396.x, 2008.

796 Verbyla, D.: Remote sensing of interannual boreal forest NDVI in relation to climatic conditions in interior Alaska,
797 *Environmental Research Letters*, 10, 10.1088/1748-9326/10/12/125016, 2015.

798 Wang, P., Huang, Q. W., Tang, Q., Chen, X. L., Yu, J. J., Pozdniakov, S. P., and Wang, T. Y.: Increasing annual and extreme
799 precipitation in permafrost-dominated Siberia during 1959-2018, *Journal of Hydrology*, 603, 10.1016/j.jhydrol.2021.126865,
800 2021.

801 Welp, L. R., Randerson, J. T., and Liu, H. P.: The sensitivity of carbon fluxes to spring warming and summer drought
802 depends on plant functional type in boreal forest ecosystems, *Agricultural and Forest Meteorology*, 147, 172-185,
803 10.1016/j.agrformet.2007.07.010, 2007.